Pharmacological Research 198 (2023) 106997

Contents lists available at ScienceDirect

Pharmacological Research

journal homepage: www.elsevier.com/locate/yphrs

Protective effect of microbiota-derived short chain fatty acids on vascular dysfunction in mice with systemic lupus erythematosus induced by toll like receptor 7 activation

Javier Moleón [a,b,1], Cristina González-Correa [a,b,1], Sofía Miñano [a,1], Iñaki Robles-Vera [c,*,2], Néstor de la Visitación [d], Antonio Manuel Barranco [a,b], Manuel Gómez-Guzmán [a,b], Manuel Sánchez [a,b], Pedro Riesco [a], Eduardo Guerra-Hernández [e], Marta Toral [a,b,f], Miguel Romero [a,b,3], Juan Duarte [a,b,f,**,3]

[a] Department of Pharmacology, School of Pharmacy and Center for Biomedical Research (CIBM), University of Granada, 18071 Granada, Spain
[b] Instituto de Investigación Biosanitaria de Granada, ibs.GRANADA, Granada, Spain
[c] Centro Nacional de Investigaciones Cardiovasculares (CNIC), Madrid 28029, Spain
[d] Division of Clinical Pharmacology, Department of Medicine, Vanderbilt University Medical Center, Nashville, Tennessee, USA
[e] Department of Nutrition and Bromatology, University of Granada, Granada, Spain
[f] Ciber de Enfermedades Cardiovasculares (CIBERCV), Spain

ARTICLE INFO

Keywords:
Hypertension
Endothelial dysfunction
Short chain fatty acids
GPR43
Immune system
Systemic lupus erythematosus

ABSTRACT

Our objective was to investigate whether short-chain fatty acids (SCFAs), specifically acetate and butyrate, could prevent vascular dysfunction and elevated blood pressure (BP) in mice with systemic lupus erythematosus (SLE) induced by TLR7 activation using imiquimod (IMQ). Treatment with both SCFAs and dietary fibers rich in resistant starch (RS) or inulin-type fructans (ITF) effectively prevented the development of hypertension and cardiac hypertrophy. Additionally, these treatments improved aortic relaxation induced by acetylcholine and mitigated vascular oxidative stress. Acetate and butyrate treatments also contributed to the maintenance of colonic integrity, reduced endotoxemia, and decreased the proportion of helper T (Th)17 cells in mesenteric lymph nodes (MLNs), blood, and aorta in TLR7-induced SLE mice. The observed changes in MLNs were correlated with increased levels of GPR43 mRNA in mice treated with acetate and increased GPR41 levels along with decreased histone deacetylase (HDAC)− 3 levels in mice treated with butyrate. Notably, the effects attributed to acetate, but not butyrate, were nullified when co-administered with the GPR43 antagonist GLPG-0974. T cell priming and differentiation into Th17 cells in MLNs, as well as increased Th17 cell infiltration, were linked to aortic endothelial dysfunction and hypertension subsequent to the transfer of faecal microbiota from IMQ-treated mice to germ-free (GF) mice. These effects were counteracted in GF mice through treatment with either acetate or butyrate. To conclude, these findings underscore the potential of SCFA consumption in averting hypertension by restoring balance to the interplay between the gut, immune system, and vascular wall in SLE induced by TLR7 activation.

1. Introduction

Individuals with SLE have a significantly higher risk of stroke and myocardial infarction than the general population, ranging from two to three times higher. The risk of myocardial infarction is especially high in premenopausal women, exceeding traditional risk estimates. One study found a 52-fold increase in myocardial infarction among women with SLE aged 35–44 years [1]. Hypertension is widely recognized as the

* Corresponding author.
** Correspondence to: Department of Pharmacology, School of Pharmacy, University of Granada, 18071 Granada, Spain.
E-mail address: jmduarte@ugr.es (J. Duarte).
[1] These authors contributed equally as first authors.
[2] iñaki.robles@cnic.es
[3] These authors contributed equally to the supervision of the study.

https://doi.org/10.1016/j.phrs.2023.106997
Received 14 September 2023; Received in revised form 10 November 2023; Accepted 13 November 2023
Available online 14 November 2023

leading risk factor for cardiac events in lupus patients [2]. According to Zhao M et al., 71.9% of SLE patients had hypertension, and a significant proportion of them, 74.4%, were either undertreated or not treated at all [3].

The engagement of Toll-like receptors (TLRs) plays a significant role in the development and advancement of systemic lupus erythematosus (SLE) in both human patients and spontaneous mouse models [4,5]. Activation of TLR7 can trigger alterations in phenotype and functionality, observed in human SLE cases, including elevated levels of autoantibodies and involvement of multiple organs [6]. Indeed, augmented TLR7 gene copies, single nucleotide polymorphisms, and the upregulation of signaling pathways downstream of TLR7 have been linked to an increased susceptibility to SLE in humans [7]. Recently, the occurrence of human SLE associated with a TLR7 gain-of-function variant has been reported [8]. TLR7 plays a crucial role in the development of lupus by promoting the production of type I interferon (IFN) [9]. Activation of TLR7 induces vascular dysfunction in non-autoimmune mice, [10] and accelerates cardiovascular pathology in mice prone to lupus [11]. Vascular dysfunction triggered by TLR7 activation is characterized by inflammation, oxidative stress, impaired endothelium-mediated relaxation, and remodeling, and is associated with elevated blood pressure (BP). These characteristics are partially mediated by interleukin (IL)−17 [12].

Notably, gut dysbiosis was identified in TLR7-dependent mouse models of SLE [13,14]. The translocation of *Lactobacillus reuteri*, a gut pathobiont, to secondary lymphoid tissue and the liver has been shown to drive autoimmunity, which can be ameliorated by consuming resistant starch (RS) in the diet. RS intake suppresses the pathological levels of *L. reuteri* and its translocation through the action of short-chain fatty acids (SCFAs) [13]. Furthermore, this dysbiotic microbiota has been implicated in the development of vascular dysfunction and hypertension by promoting the differentiation of Th17 cells in the gut's secondary lymph nodes and their subsequent infiltration into the vascular wall [12]. Interestingly, the consumption of probiotic has been shown to prevent vascular dysfunction in lupus mice by reducing Th17 polarization [14]. The gut microbiota and their metabolites play a critical role in regulating the host immune system. Intestinal bacteria produce lipopolysaccharide (LPS) and SCFAs, which have opposing effects on T cell polarization and inflammation, increasing, and reducing them, respectively [15]. Numerous commensal gut bacteria can produce SCFAs, including acetate by some bacteria, butyrate by *Clostridium* species, and propionate by *Akkermansia*. However, there have been no significant findings indicating alterations in SCFA-producing bacteria in TLR7-induced lupus mice, suggesting that reduced levels of SCFAs may not contribute to vascular dysfunction in SLE [12,14]. Conversely, SCFAs have been shown to enhance vascular function and reduce BP in non-lupus-prone rodents [16–23], as well as in humans characterized by SCFAs depletion in the gut [24]. Moreover, SCFAs supplementation reduced plasma anti-ds-DNA in TLR7.1 Tg C57Bl/6 mice [13], which can attenuate SLE hypertension [25]. In fact, our recent study demonstrated that consuming fiber improved vascular function in a polygenetic lupus model, potentially by increasing SCFAs production [26]. SCFAs exert their regulatory effects on immune and endothelial function through the inhibition of histone deacetylases (HDACs) and/or the activation of G-protein coupled receptors (GPRs), specifically GPR41 (also known as free fatty acid receptor 3, FFAR3) and GPR43 (or FFAR2) [27,28]. However, the expression of GPR41 and GPR43 varies across different cell types. GPR41 is predominantly expressed in endothelial cells, while GPR43 is more prevalent in immune cells [29]. Butyrate exhibits stronger activity on GPR41, propionate acts as the most potent agonist for both GPR41 and GPR43, and acetate displays greater selectivity for GPR43 [30]. Furthermore, butyrate and propionate, but not acetate, can function as HDAC inhibitors [31]. However, the expression levels of GPRs and HDACs in the gut, secondary lymph nodes, and vascular wall of TLR7-induced lupus mice have yet to be investigated, as this may determine the response to SCFAs. Given that SCFAs inhibit immune and inflammatory pathways, our objective was to examine whether SCFAs, specifically acetate and butyrate, can prevent vascular dysfunction and elevated BP in TLR7-induced lupus mice and assess the potential involvement of HDACs and/or GPRs as underlying mechanisms.Principio del formulario.

2. Material and methods

2.1. Animals and experimental groups

We adhered to the animal protocols outlined in the National Institutes of Health Guide for the Care and Use of Laboratory Animals, and we obtained approval from the Ethics Committee of Laboratory Animals at the University of Granada, Spain (Reference: 12/11/2017/164). Additionally, our procedure followed the guidelines outlined in the Transparency on Gut Microbiome Studies in Essential and Experimental Hypertension [32], as well as the ARRIVE guidelines [33]. We specifically opted to use female mice due to their heightened susceptibility to TLR7-driven functional responses and autoimmunity [34]. Additionally, lupus is more prevalent in women, further supporting our choice.

For *Experiment 1*, we selected female BALB/cJRj mice aged seven to nine weeks, procured from Janvier (Le Genest, France). Mice were divided into four experimental groups (n = 8 each): an untreated control group (CTR), a group treated with imiquimod (IMQ), an IMQ-treated group supplemented with magnesium acetate (68 mM, IMQ-ACE), and an IMQ-treated group supplemented with sodium butyrate (40 mM, IMQ-BUT) in their drinking water [13]. All mice were provided a standard chow diet (SAFE A04, Augy, France) and were randomly assigned to receive either regular drinking water (CTR and IMQ groups) or drinking water enriched with SCFAs. Considering the bitterness of butyrate, a sweetener (Equal, 4 g/l) was added to the water of all experimental groups. Freshwater bottles were replenished daily, and we monitored and controlled water and food consumption for all groups on a daily basis. IMQ-treated mice were subjected to a total of 1.25 mg of IMQ (Zyclara® 3.75% cream) from Laboratories Meda Pharma S.A.U. (Madrid, Spain) applied to their right ears three times per week on alternate days over 8 weeks. This topical IMQ application to the skin effectively triggers the development of systemic autoimmune disease [6], justifying its application to induce a murine model resembling SLE.

Certain types of fiber undergo fermentation by gut microbiota, leading to the production of SCFAs as byproducts. Prior studies utilizing experimental models have reported the beneficial effects of dietary fiber in reducing BP, largely attributed to SCFAs [16]. In our investigation of the role of dietary SCFAs, we introduced two distinct fiber sources: inulin-type fructans (ITF) and RS, both known to yield SCFAs. Alongside the control groups, we included two sets of IMQ-treated mice: IMQ-RS (IMQ mice treated with SF11–025 diet: 72.7% insoluble fiber, sourced from Specialty Feeds, Perth, Australia) (n = 8) [16], and IMQ-ITF (SLE mice treated with ORAFTI P95, a soluble fiber from Beneo, Tener, Belgium) (n = 8) [35]. Insoluble fiber was provided as standard pellets, while soluble fiber was diluted in drinking water at a final dose of 250 mg/mouse/day.

Throughout this experiment, all animals were housed within specific pathogen-free (SPF) facilities at the University of Granada's Biological Services Unit, adhering to standard laboratory conditions that include a 12-hour light/dark cycle, temperature maintained between 21 and 22ºC, and humidity levels between 50% and 70%. To prevent horizontal bacterial transmission, the mice were individually housed in Makrolon cages (Ehret, Emmerdingen, Germany) and furnished with dust-free laboratory bedding and enrichment items. The study design ensured equal group sizes and sufficient statistical power. Random allocation of animals into experimental groups was conducted, and the researcher remained blinded to SCFAs and fiber treatments until completion of data analysis.

Experiment 2: To investigate the role of GPR43 in the protective effects of SCFAs in IMQ-induced lupus, we introduced two additional

groups of IMQ mice co-treated with SCFAs and the GPR43 antagonists GLPG-0974 (Tocris Bioscience, Bristol, UK) [36]: IMQ-ACE-GPLG and IMQ-BUT-GPLG. A stock solution of GLPG-0974 was prepared by dissolving it in 0.1% dimethyl sulfoxide (DMSO). GLPG-0974 (1 mg/kg body weight) was then diluted in saline and daily administered at a volume of 100 μL via oral gavage [37]. The untreated IMQ group received the vehicle.

Experiment 3: To investigate the potential impact of the microbiota on BP regulation, we conducted a faecal inoculation study using germ-free (GF) female C57Bl/6 J mice aged ten weeks, procured from the University of Granada, Spain [38]. In this process, fresh stool samples were collected individually from mice belonging to the CTR and IMQ groups in Experiment 1. These samples were combined to create a bacterial suspension by vigorous vortexing at a 1:20 ratio in sterile phosphate-buffered saline (PBS). The suspension was then subjected to centrifugation at 60 g for 5 min to eliminate any debris. The resulting suspension was divided into aliquots and stored at − 80ºC. Subsequently, the mice were randomly divided into four groups: GF mice with CTR microbiota (GF-CTR) (n = 8), and GF mice with IMQ microbiota (GF-IMQ) (n = 24). The GF mice with IMQ microbiota were further subdivided into three groups: vehicle (GF-IMQ) (n = 8), magnesium acetate (68 mM, GF-IMQ-ACE) (n = 8), or sodium butyrate (40 mM, GF-IMQ-BUT) (n = 8), administered through their drinking water. The inoculation was carried out twice consecutively during the first week, followed by a monitoring period of 3 weeks. Throughout the study, all GF mice were housed under sterile conditions within a gnotobiotic facility and were provided ad libitum access to a standard laboratory diet. Microbiota inoculation was performed under sterile conditions in gnotobiotic facilities. After 3 weeks, stool samples were collected from all experimental groups and fully homogenized in PBS. 100 μL of the resultant material were cultured in chocolate agar plates for 24 h at 37 °C 5% CO_2 [39]. Presence of any colony forming units (CFU) was considered as a positive transplant control.

2.2. Blood pressure measurements, physical characteristics, and heart and kidney weight indices

Systolic blood pressure (SBP) measurements were acquired from conscious mice that were pre-warmed at 35ºC for 10–15 min and gently restrained for tail-cuff plethysmography (Digital Pressure Meter, LE 5001; Letica S.A., Barcelona, Spain). Mice underwent a familiarization process, and the replication count was consistent with prior reports [38]. Body weights across all groups were recorded in grams. To derive the left ventricle, liver, spleen, and kidney weight indices, respective weights were normalized by the tibia length. Following measurements, samples were promptly cryopreserved in liquid nitrogen and stored at − 80ºC.

2.3. Plasma, urine, and faecal parameters

At the designated endpoints of the experiments, all animals were euthanized under isoflurane anesthesia. Plasma was obtained from collected blood samples, and levels of anti-ds-DNA antibodies were assessed using an Alpha Diagnostic ELISA Kit (Alpha Diagnostic International, San Antonio, Texas, USA) following the provided guidelines, as previously documented [12]. Additionally, we quantified plasma LPS content using the PierceTM chromogenic endotoxin quant kit (Thermo Fisher Scientific, Illinois, USA), according to manufacturer's instructions.

Concentrations of SCFAs in mouse plasma and faecal samples were measured through gas chromatography, employing a previously reported methodology [21].

2.4. Vascular reactivity studies

Segments of the aorta were mounted in a wire myograph (model 610 M, Danish Myo Technology, Aarhus, Denmark) containing Krebs solution, and subjected to standard conditions for isometric tension measurement, as detailed in prior publications from our research group [38]. Pre-contraction was induced using thromboxane A_2 analog U46619 (3 nM). Serial relaxation curves were generated over 30 min, alternating between washes in the absence and presence of the specific pan-NOX inhibitor VAS2870 (10 μM) or the Rho kinase inhibitor Y27632 (0.5 μM). To assess the role of IL-17, aortic rings were exposed to anti-IL-17a antibody (10 μg/mL) for 6 h prior to constructing a relaxation-response curve with acetylcholine. Results were expressed as relaxation levels relative to pre-contraction tone.

2.5. NADPH oxidase activity

NADPH oxidase activity was assessed in vascular tissue via a lucigenin-enhanced chemiluminescence assay conducted in intact aortic segments, following established methods [12]. Aortic segments from all experimental groups were incubated at 37 ºC in HEPES-based solution for 30 min, with NADPH (100 μM) added to stimulate enzymatic activity. Measurements were recorded using a scintillation chamber (Lumat LB 9507, Berthold, Germany) in the presence of lucigenin (5 μM). NADPH oxidase activity was quantified as relative luminescence units (RLU) per minute per milligram of dry aortic tissue.

2.6. Reverse transcriptase-polymerase chain reaction (RT-PCR) analysis

RNA samples were extracted from the colon, mesenteric lymph nodes (MLNs), and aorta through homogenization, followed by cDNA retrotranscription using standard RT-PCR methods. Tissues were homogenized in 0.5 mL of PRImeZOL Reagent (Canvax Biotech, S.L., Córdoba, Spain), following previous protocols [10]. PCRs were executed using a PCRMax Eco 48 thermal cycler (PCRMax, Stone, Staffordshire, UK). For mRNA expression analysis, quantitative real-time RT-PCR technique was employed. Forward and reverse primers used in PCR reactions are detailed in Table S1. RT-PCRs were conducted as per our established protocol, with ribosomal protein L13a (*Rpl13a*) as the reference gene. Data analysis was carried out using the ΔΔCt method [10].

2.7. Flow cytometry

MLNs, spleens, and aorta were dissected, homogenized, and filtered to eliminate tissue debris. Blood was also collected. Erythrocytes were lysed using Gey's solution. For optimal detection of intracellular cytokines via flow cytometry, a protein transport inhibitor (BD GolgiPlugTM) was applied following the manufacturer's instructions, along with 50 ng/mL phorbol 12-myristate 13-acetate and 1 μg/mL ionomycin. To prevent nonspecific binding, anti-Fc-γ receptor antibodies from Miltenyi Biotec were employed. Cells were then stained for B cells (CD45 +, B220 +), Th17 cells (CD45 +, CD3 + CD4 +, IL-17A+), Th1 cells (CD45 +, CD3 + CD4 +, interferon (IFN)γ), and regulatory T cells (Tregs) (CD45 +, CD3 +, CD4 +, CD25 +). Essential antibodies used for flow cytometry are enumerated in Table S2. Flow cytometric analysis was conducted on a BD FACSymphony™ A5 Cell Analyzer (BD Biosciences), following established methods [12,38], with the gating strategy outlined in Fig. S1.

2.8. DNA extraction, 16 S rRNA gene amplification, bioinformatics

DNA was extracted from stool samples using previously described techniques [40]. Amplification of the V3-V4 region of the 16 S rRNA gene was performed on these samples [41]. Amplicons were analyzed and quantified using a Bioanalyzer 2100 (Agilent). Subsequently, samples underwent paired-end sequencing (2 ×300) on an Illumina MiSeq instrument at Unidad de Genómica (Parque Científico de Madrid, Madrid, Spain).

To process raw sequences, the barcoded Illumina paired-end sequencing (BIPES) pipeline along with BIPES protocols were utilized

[42,43]. UCHIME in de novo mode (using-minchunk 20-xn 7-noskipgaps 2) was employed to identify and remove chimeras [44]. Subsequent analyses employed 16 S Metagenomics (Version: 1.0.1.0) from Illumina. Sequences were clustered into operational taxonomic units (OTUs) with USEARCH, applying a threshold distance of 0.03 to classify sequences with 97% similarity into the same OTU. Representative sequences were aligned using PyNAST with SILVA database as the template file. The Ribosome Database Project (RDP) algorithm was used to classify representative sequences into specific taxa [45]. Taxonomy classification used the Taxonomy Database from the National Center for Biotechnology Information. Bacteria were classified based on SCFAs end-products, as described earlier [46]. Predicted metagenomes were mapped to the Kyoto Encyclopedia of Genes and Genomes pathways (KEGG) using the phylogenetic investigation of communities by reconstruction of unobserved states (PICRUSt) method. KEGG module abundance was determined by aggregating the abundance of genes annotated to the same feature. Pathway results were presented as the relative abundance of predicted functions.

2.9. Statistical analysis

Shannon diversity, Chao richness, Pielou evenness, and observed species indexes were calculated using Palaeontological Statistics software (PAST 4.02). OTU reads were normalized to total reads in each sample. Taxonomic differences between experimental groups were assessed using Partial Least Square Discriminant Analysis (PLS-DA) on the data. Data analysis was performed with GraphPad Prism 8. Results are presented as means ± SEM. For tail SBP evolution and concentration-response curves to acetylcholine, two-way repeated-measures analysis of variance (ANOVA) with Bonferroni post hoc test was employed. Other variables were assessed for normality using the Shapiro-Wilk normality test. For normally distributed data, one-way ANOVA and Tukey post hoc test were used. For non-normally distributed data, Mann-Whitney test or Kruskal-Wallis test with Dunn's multiple comparison test was applied. Statistical significance was considered at $P < 0.05$.

3. Results

3.1. SCFA treatments prevented the increase in blood pressure and target organ hypertrophy, but not disease activity in lupus-prone mice

We examined whether the administration of SCFAs induced alterations in gut microbiota composition. Our findings revealed that IMQ treatment reduced various microecological parameters of alpha-diversity (ACE, Shannon, and Simpson) (Fig. S2A) and led to changes in beta-diversity (Fig. S2B). However, neither acetate nor butyrate administration modified these parameters or the relative abundance of bacteria belonging to different phyla (Fig. S2C). SCFAs induced minor changes in certain genera (both acetate and butyrate reduced

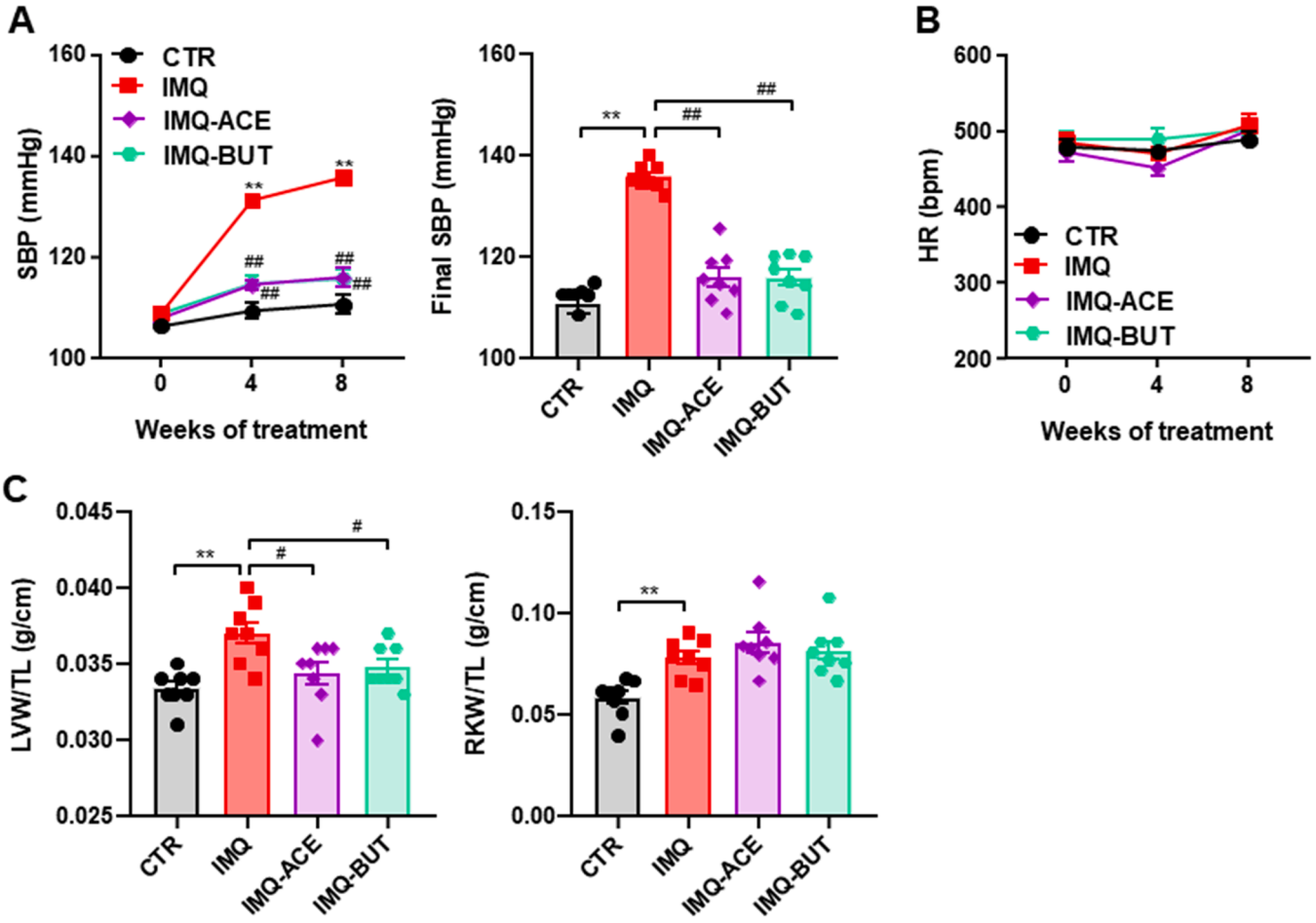

Fig. 1. Effects of SCFA treatments on blood pressure and target organ hypertrophy in TLR7-induced lupus mice. (A) Time-course and final systolic blood pressure (SBP), and (B) heart rate (HR) measured through tail-cuff plethysmography. (C) Morphological parameters: left ventricle weight (LVW) and right kidney weight (RKW) normalized by tibia length (TL) in control (CTR), imiquimod (IMQ), and IMQ-treated mice with acetate (ACE) or butyrate (BUT). Data presented as means ± SEM (n = 8). Two-way ANOVA with Sidak's multiple comparisons test for SBP and HR. One-way ANOVA and Tukey's post hoc or Kruskal-Wallis with Dunn's multiple comparisons for final SBP and morphological variables. * *P < 0.01 vs. CTR; #P < 0.05 and ##P < 0.01 vs. untreated IMQ.

Alkaliphilus, Akkermansia, and *Faecalibacterium*; acetate increased *Bacillus*, and butyrate increased *Selenomonas*) (Fig. S2D) and bacterial metabolic pathways (butyrate increased ribokinase and decreased penicillin-binding protein compared to the IMQ group; no significant changes were induced by acetate) (Fig. S2E), suggesting that SCFAs exert direct effects on host target organs rather than mediated by changes in gut microbiota.

As expected, TLR7 activation with IMQ resulted in a gradual increase in SBP, with the IMQ group showing approximately 25 mmHg higher than control animals at the end of the experiment. Both acetate and butyrate inhibited the development of high BP induced by IMQ by approximately 78.9% and 79.3%, respectively (Fig. 1A). However, no significant differences in heart rate were found between the CTR and IMQ groups, and both SCFAs treatments did not alter heart rate (Fig. 1B). Sustained high BP is a crucial factor in the development of cardiac and renal hypertrophy [47]. We observed that IMQ-treated mice exhibited higher left ventricular weight/tibia length and right kidney weight/tibia length (approximately 10% and 34%, respectively) than control mice, indicating that IMQ induced cardiac and renal hypertrophy. Both SCFAs prevented left ventricular hypertrophy, but not renal hypertrophy (Fig. 1C), suggesting that factors other than BP might be contributing to kidney hypertrophy in this lupus model, which appeared to be unaffected by SCFAs.

In this TLR7-mediated autoimmunity model, increased plasma levels of autoantibodies, splenomegaly, hepatomegaly, and higher type-1 IFN expression in lymph organs were observed [6,9]. In fact, we found elevated plasma levels of anti-dsDNA (Fig. S3A), spleen weight/tibia length (Fig. S3B), liver weight/tibia length (Fig. S3C), and *Ifnα* mRNA levels in MLNs (Fig. S3D) in IMQ mice compared to the CTR group. However, both SCFAs were unable to reduce these signs of autoimmunity in IMQ mice. Additionally, we evaluated the immunomodulatory effects of SCFAs by measuring the levels of B cells in MLNs and spleens after TLR7 activation. IMQ treatment increased the percentage of B cells in the spleen but not in MLNs, and both SCFAs treatments had no effect on B cell content (Fig. S3E). In addition, splenic total T cells and Tregs proportion was reduced and increased by IMQ, respectively, and unchanged by SCFAs, whereas IMQ increased the percentage of Th17, which was reduced by both SCFAs (Fig. S4).

3.2. SCFA treatments prevented endothelial dysfunction, vascular oxidative stress and Th17 infiltration in aorta

Aortas from the IMQ group exhibited significantly reduced endothelium-dependent vasorelaxant responses to acetylcholine compared to the CTR group (Emax reduced by 34%, $P < 0.01$) (Fig. 2A). However, treatment with both acetate and butyrate reversed the impairment of acetylcholine-induced relaxation. The acetylcholine-induced response was also improved in the IMQ group after incubation with the pan-NOX inhibitor VAS2870, indicating mediation by NADPH oxidase activation, and by the Rho kinase inhibitor Y27632 (Fig. 2A), suggesting that the impaired acetylcholine-induced relaxation is, at least in part, due to Rho kinase activation. Previous studies have

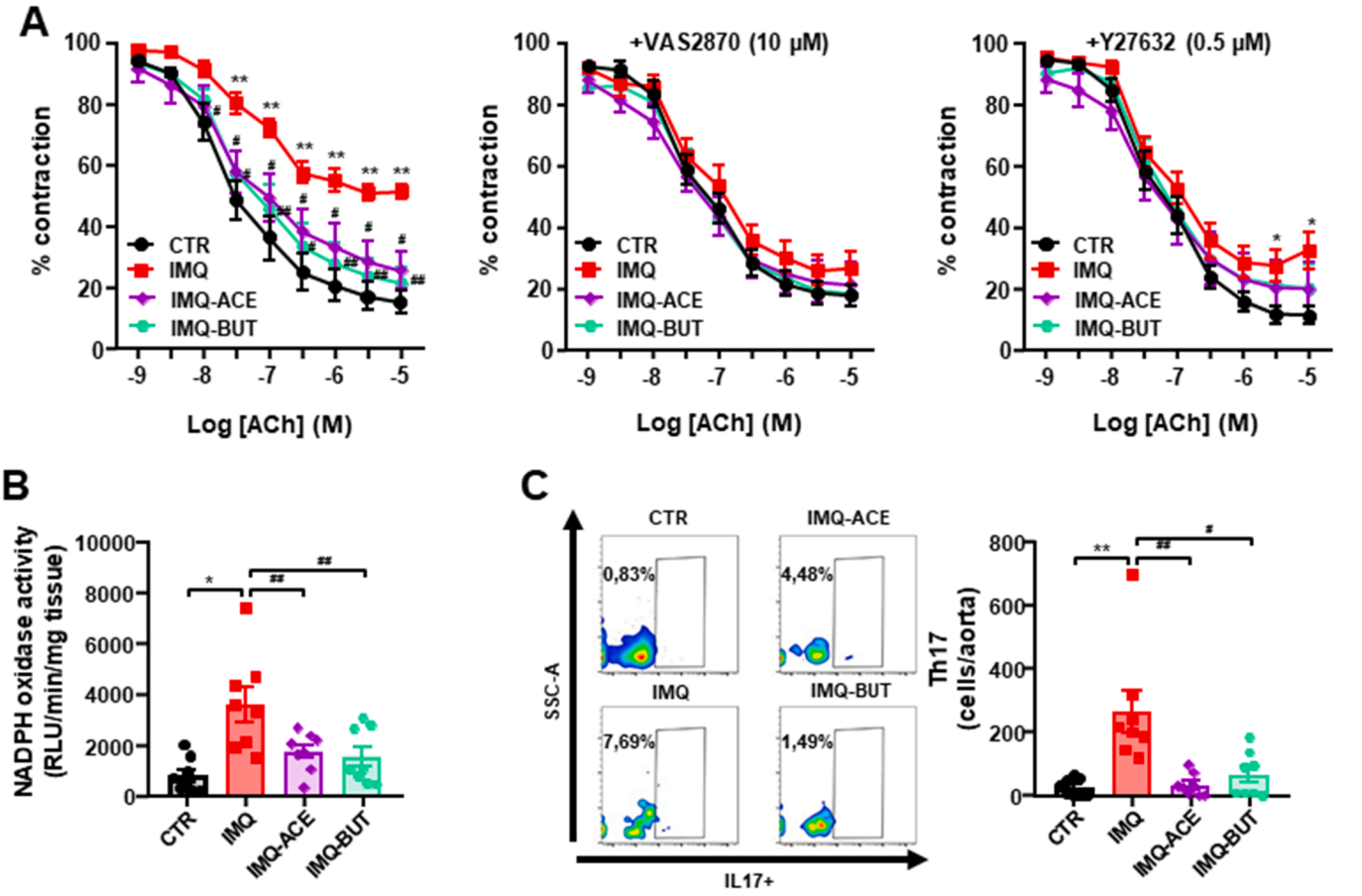

Fig. 2. Effects of SCFA treatments on endothelial function, NADPH oxidase activity, and immune cell infiltration in TLR7-induced lupus mice. (A) Vascular relaxation responses induced by acetylcholine (ACh) in aortic rings pre-contracted by U46619, with or without NADPH oxidase inhibitor VAS2870 or Rho kinase inhibitor Y27632. (B) Aortic NADPH oxidase activity. (C) Aortic immune cell infiltration measured by flow cytometry. Groups: control (CTR), imiquimod (IMQ), and IMQ-treated mice with acetate (ACE) or butyrate (BUT). Data presented as means ± SEM (n = 8). Two-way ANOVA with Sidak's multiple comparisons for ACh concentration-response curves. One-way ANOVA and Tukey's post hoc or Kruskal-Wallis with Dunn's multiple comparisons for other variables. *$P < 0.05$ and * *$P < 0.01$ vs. CTR; #$P < 0.05$ and ##$P < 0.01$ vs. untreated IMQ.

indicated a link between reactive oxygen species (ROS)-dependent activation of RhoA/Rho kinase [48]. As the primary source of ROS in the vascular wall, NADPH oxidase activity was approximately 4.5-fold higher in the aortic rings from the IMQ group compared to the CTR group, and both acetate and butyrate reduced this increased activity by around 66% and 73%, respectively (Fig. 2B). Inflammatory cells have been demonstrated to enhance vascular ROS synthesis [49]. We further investigated T lymphocyte extravasation in the aorta and observed that Th17 cells were approximately 10-fold higher in the aortas of the IMQ group compared to the CTR group; however, this increase was mitigated by both acetate and butyrate treatment (Fig. 2C).

3.3. *Fiber treatments increased SCFAs production by remodeling the gut microbiota and prevented the rise in blood pressure*

The consumption of dietary fiber induced significant and profound changes in the composition of the gut microbiota. In IMQ mice, RS led to a reduction in Chao richness but a normalization of Shannon and Simpson diversity (Fig. 3**A**). We conducted a two-dimensional PCoA analysis of the bacterial community, which measures microorganism diversity among samples (β-diversity) at various taxonomic levels (phylum, class, order, family, genus, and species). The Permanova analysis showed a significant clustering of the animals into each group (Fig. 3B). Specifically, bacteria belonging to Actinobacteria, Firmicutes, and Verrucomicrobia were reduced in the IMQ group compared to the CTR group, whereas those belonging to Bacteroidetes were increased (Fig. 3C, Fig. S5). RS treatment reduced the relative abundance of Firmicutes and increased Bacteroidetes and Verrucomicrobia, while ITF did not significantly change the microbiota composition at the phylum level (Fig. 3C, Fig. S5). Consequently, the Firmicutes/Bacteroidetes (F/B) ratio, an index of gut dysbiosis, was reduced by IMQ and increased by RS treatment (Fig. 3D). At the family level, we observed reduced *Bacillaceae* and *Verrumicrobiaceae* and increased *Porphyromonadaceae* relative abundance in the IMQ group compared to the CTR group (Fig. S5, S6). RS treatment increased *Bacillaceae* and *Verrucomicrobiaceae* proportions and reduced *Porphyromonadaceae* and *Prevotellaceae*, whereas ITF consumption increased *Bacteroidaceae* and reduced *Barnesiella* and *Porphyromonas* (Fig. S5, S6). At the genus level, we found a lower relative abundance of *Akkermansia* and *Bacillus* and a higher abundance of *Barnesiella* in the IMQ group compared to the CTR group (Fig. S5, S7). RS treatment increased *Akkermansia*, *Bacillus*, and *Clostridium*, and reduced *Alkaliphilus, Barnesiella, Porphyromonas*, and *Prevotella*, whereas ITF increased *Bacteroides* and reduced *Barnesiella* and *Porphyromonas* (Fig. S5, S7).

As prebiotic fiber is fermented by gut bacteria, leading to the production of SCFAs, we investigated the relative abundance of SCFAs-

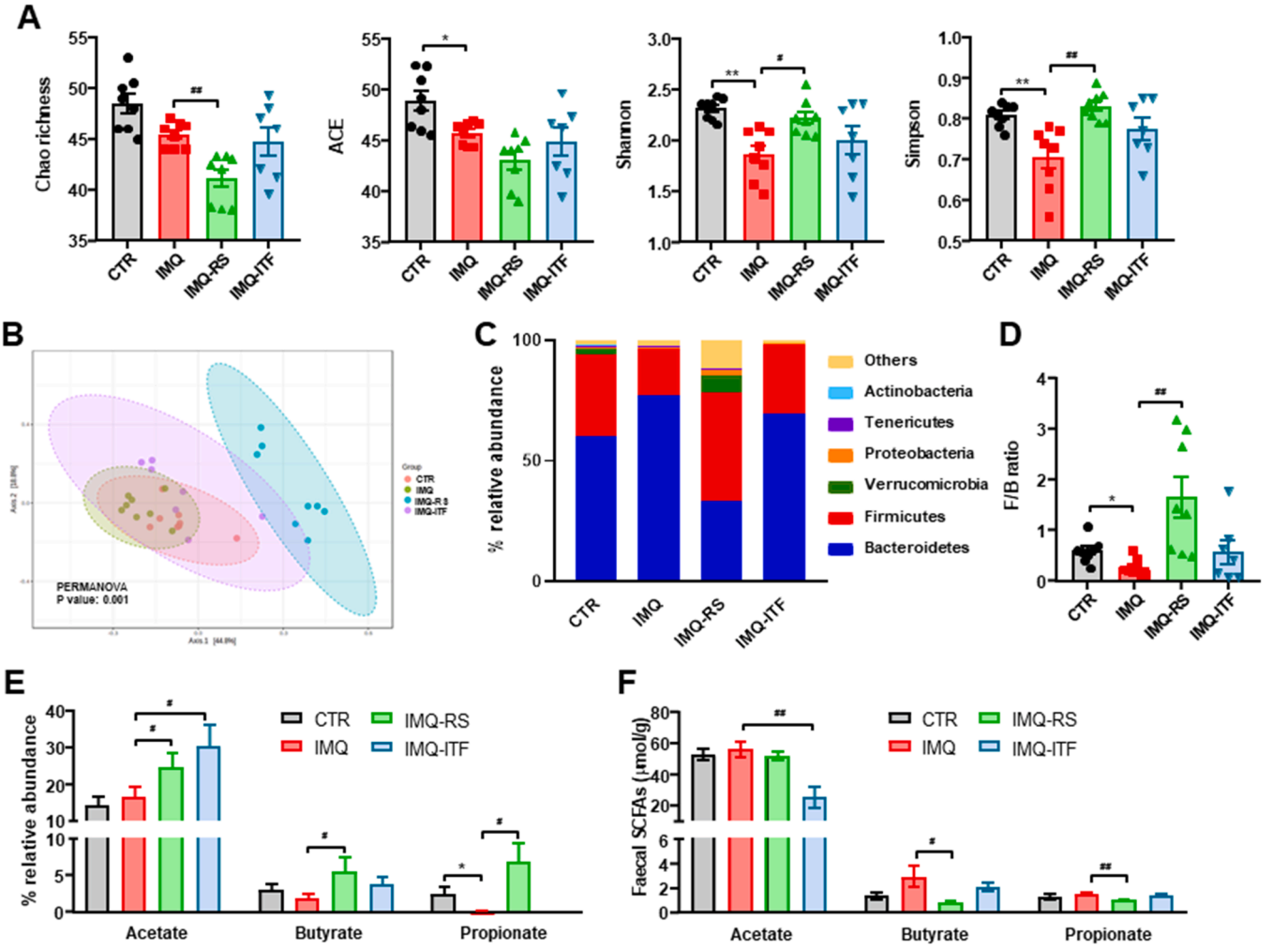

Fig. 3. Effects of fiber treatments on gut microbiota composition in TLR7-induced lupus mice. (A) Alpha diversity indices, (B) Principal Coordinate Analysis (PCoA) of gut microbiota, (C) Proportion of bacterial phyla, (D) Firmicutes/Bacteroidetes (F/B) ratio, and (E) Proportion of short-chain fatty acids (SCFAs)-producing bacteria in feces using 16 S rRNA analysis. (F) SCFAs concentrations in feces measured by gas chromatography. Groups: control (CTR), imiquimod (IMQ), IMQ treated with resistant starch (RS) or inulin-type fructans (ITF). Data presented as means ± SEM (n = 8). One-way ANOVA and Tukey's post hoc or Kruskal-Wallis with Dunn's multiple comparisons for all variables.

producing bacteria. We observed no significant changes in acetate- and butyrate-producing bacteria, but there was a decreased abundance of propionate-producing bacteria in the IMQ group compared to the CTR group (Fig. 3E). However, the RS diet elevated the proportion of bacteria producing acetate, butyrate, and propionate, while ITF increased only the proportion of acetate-producing bacteria (Fig. 3E). Notably, the faecal content of propionate and butyrate in the IMQ-RS group was lower compared to the IMQ group, although acetate content remained unchanged. Furthermore, in ITF-treated mice, the faecal acetate content was lower than that in IMQ mice (Fig. 3F), indicating enhanced SCFAs absorption in the fiber-treated groups.

SCFAs possess the capability to enter the cytosol through passive diffusion and can also be absorbed by solute transporters, such as the proton-coupled monocarboxylate transporters (MCT)1 and MCT4, which are upregulated due to prolonged acetate or butyrate consumption [50]. This elucidates our findings, as both fiber treatments increased the presence of SCFAs-producing bacteria in IMQ mice and resulted in higher colonic mRNA levels of *Mct1* and *Mct4* (Fig. S8A). Moreover, butyrate within intestinal epithelial cells consumes local oxygen, stabilizing the hypoxia-inducible factor (HIF), a transcription factor that orchestrates barrier protection [51]. In alignment with the augmented butyrate production and absorption in the colon stemming from RS consumption, we observed elevated colonic *Hif-1* mRNA levels in RS-treated mice compared to the IMQ group (Fig. S8B).

Similar to SCFAs treatments, both RS and ITF consumption effectively prevented the rise in SBP to a similar extent (approximately 69.4% and 66.4%, respectively) (Fig. 4A). Additionally, both RS and ITF reduced left ventricular hypertrophy (Fig. 4B), increased endothelium-dependent aortic relaxation in response to acetylcholine (Fig. 4C) and achieved these effects by reducing NADPH oxidase activity (Fig. 4D) and Th17 infiltration (Fig. 4E). In contrast to the consumption of acetate or butyrate alone, RS fiber, which increased the bacterial production of acetate, butyrate, and propionate, showed greater efficacy in improving the main signs of autoimmunity in this model, such as high plasma anti-ds-DNA levels (Fig. S9A), splenomegaly (Fig. S9B), hepatomegaly (Fig. S9C), and elevated mRNA levels of *Ifnα* in MLNs (Fig. S9D). However, ITF fiber did not exhibit significant effects in these parameters. Moreover, neither RS nor ITF had any impact on B cell content in MLNs and spleen (Fig. S9E).

3.4. SCFA treatments improved intestinal integrity and inflammation

Recognizing the importance of the translocation of the structural bacterial component LPS in relation to autoimmunity and high BP [52], we proceeded to evaluate the integrity and permeability of the intestinal epithelium. We assessed gut barrier integrity by examining colonic mRNA expression of key junctional transcripts (Fig. 5A), including occludin (*Ocln*) and zonula occludens-1 (*Zo-1*), along with mucin molecules (Fig. 5B), such as mucin-2 (*Muc-2*) and *Muc-3*. We found that mRNA levels of *Ocln* were lower (approximately 54%) in the IMQ group compared to the CTR group, while no significant changes were observed in the other markers of gut integrity. This discrepancy resulted in an

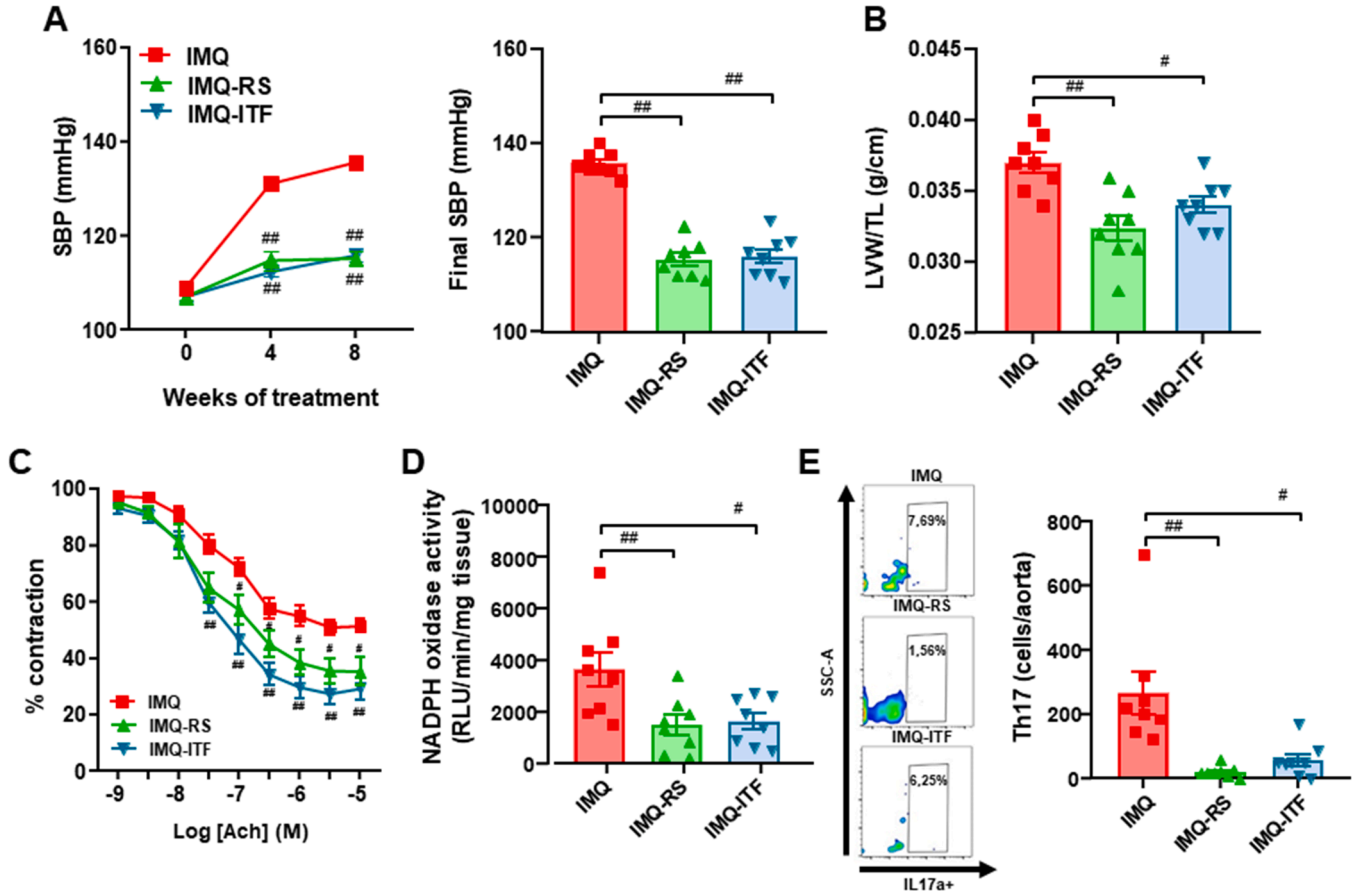

Fig. 4. Effects of fiber treatments on blood pressure, organ hypertrophy, endothelial function, NADPH oxidase activity, and immune cell infiltration in TLR7-induced lupus mice. (A) Time-course and final systolic blood pressure (SBP), (B) left ventricular weight (LVW) normalized by tibia length (TL), (C) acetylcholine (Ach)-induced vascular relaxation, (D) aortic NADPH oxidase activity, and (E) aortic immune cell infiltration. Groups: control (CTR), imiquimod (IMQ), IMQ treated with resistant starch (RS) or inulin-type fructans (ITF). Data presented as means ± SEM (n = 8). Two-way ANOVA with Sidak's multiple comparisons for SBP time-course and ACh concentration-response curves. One-way ANOVA and Tukey's post hoc or Kruskal-Wallis with Dunn's multiple comparisons for other variables. #P < 0.05 and ##P < 0.01 vs. untreated IMQ.

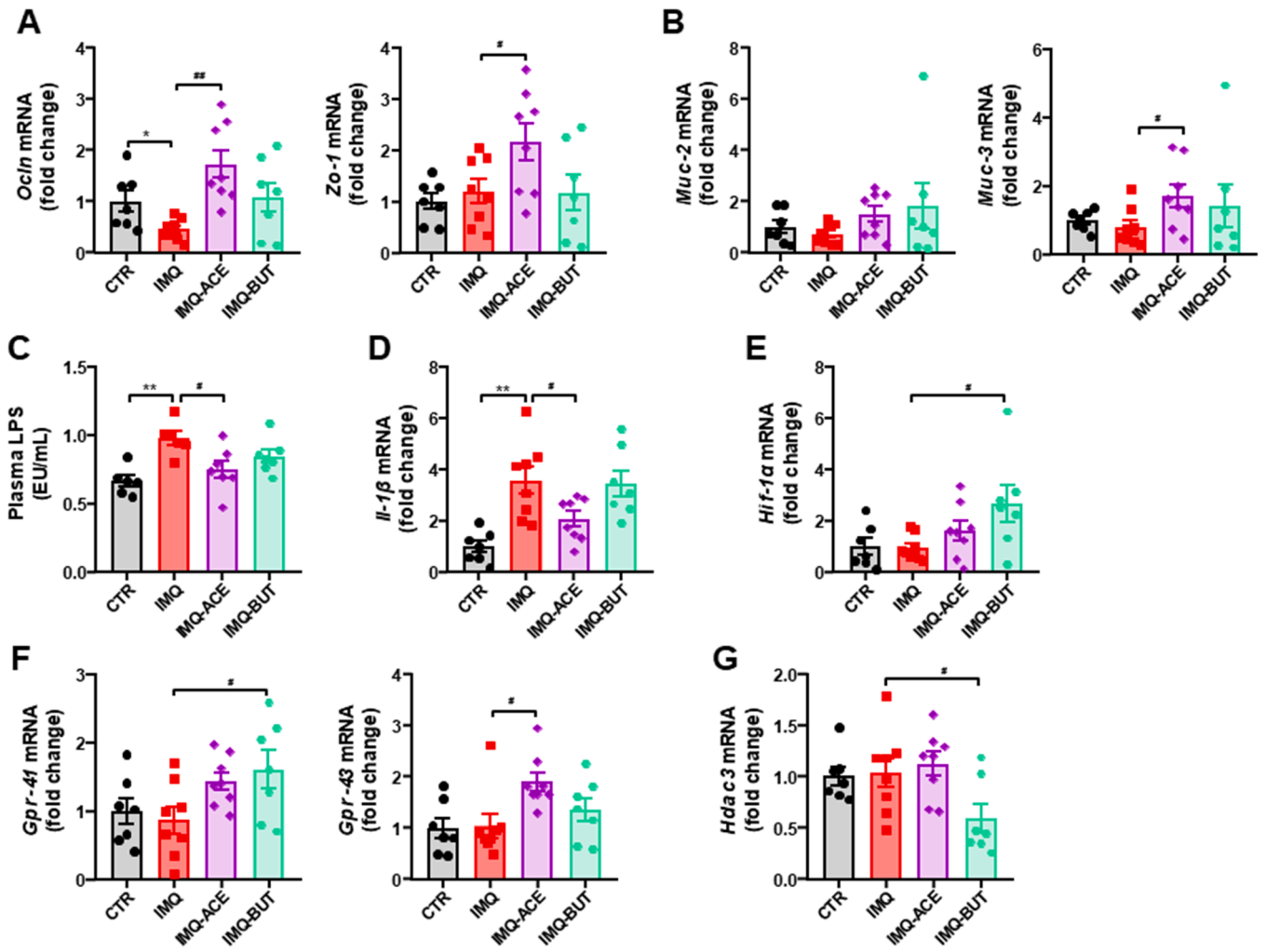

Fig. 5. Effects of SCFA treatments on colonic integrity markers, permeability, and inflammation in TLR7-induced lupus mice. (A) Colonic mRNA expression of occludin (*Ocln*) and zonula occludens-1 (*Zo-1*), and (B) mucin *(Muc)− 2* and *Muc-3* mucins. (C) Plasma LPS levels, (D) colonic interleukin *(Il)− 1β* mRNA expression, and (E) colonic hypoxia inducible factor *(Hif)− 1α* mRNA expression. (F) Colonic G-protein-coupled receptor *(Gpr)41*, *Gpr43*, and (G) histone deacetylase *(Hdac)3* mRNA levels. Groups: control (CTR), imiquimod (IMQ), and IMQ-treated mice with acetate (ACE) or butyrate (BUT). Data presented as means ± SEM (n = 8). One-way ANOVA and Tukey's post hoc or Kruskal-Wallis with Dunn's multiple comparisons for all variables. *P < 0.05 and * *P < 0.01 vs. CTR; #P < 0.05 and ##P < 0.01 vs. untreated IMQ.

increase (approximately 47%) in plasma LPS levels (Fig. 5C).

Under our experimental conditions, acetate treatment increased colonic mRNA levels of *Ocln*, *Zo-1*, and *Muc-3*, leading to a reduction in plasma endotoxin levels. However, butyrate did not demonstrate improvement in gut integrity or permeability. Furthermore, acetate treatment resulted in decreased mRNA levels of the proinflammatory cytokine interleukin *(Il)− 1β* (Fig. 5D). In contrast, butyrate acted as a primary energy source for colonocytes, consuming oxygen and stabilizing *Hif-1α* (Fig. 5E). In both epithelial and immune cells, SCFAs serve as ligands for GPRs, such as GPR43 and GPR41, which are upregulated by SCFAs or have inhibitory effects on HDAC activity. This mechanism triggers histone acetylation and modulates gene regulation involved in cell proliferation, differentiation, and the inflammatory response, contributing to intestinal homeostasis [51]. In line with this, we found elevated *Gpr41* and *Gpr43* mRNA levels in colonic samples from the IMQ-ACE and IMQ-BUT groups, respectively, compared to the IMQ mice (Fig. 5F). Additionally, colonic *Hdac3* transcript levels were down-regulated in the IMQ-BUT group compared to the IMQ mice (Fig. 5G). In summary, our findings indicate enhanced colonic integrity and reduced permeability and inflammation resulting from acetate treatment, which is associated with GPR43 activation. On the other hand, GPR41 activation and HDAC inhibition by butyrate primarily might contribute to improved colonic metabolism.

3.5. SCFA treatments attenuated T cells imbalance in MLNs

Considering the critical role of Th17 polarization in secondary lymph organs and Th17 infiltration in the aorta, which contributes to vascular alterations caused by TLR-7 activation, [10,12] we investigated whether SCFAs could modulate this Th imbalance in MLNs, as previously described in systemic hypertension [21]. Meanwhile, total T cells showed no significant changes among all experimental groups (not shown). In our study, we observed that the percentage of Th17 cells (CD4 + IL-17a+) and Th1 cells (CD4 + IFN-γ +) increased by approximately 3.2-fold and 2.5-fold, respectively, in IMQ mice, while Treg cells (CD4 + CD25 +) remained unchanged (Fig. 6). Both acetate and butyrate consumption normalized the proportion of Th17 cells without affecting Th1 and Treg cells. To gain further insights into the immunomodulatory effects of SCFAs in MLNs, we investigated the cells and cytokines involved in the polarization of Th17 cells. In IMQ mice, the integrity of the colon was compromised, enabling bacterial translocation through the intestinal barrier and triggering the activation and migration of CX3CR1 + cells, such as dendritic cells or macrophages, towards the lower intestinal tract lymph nodes [53]. These cells also present

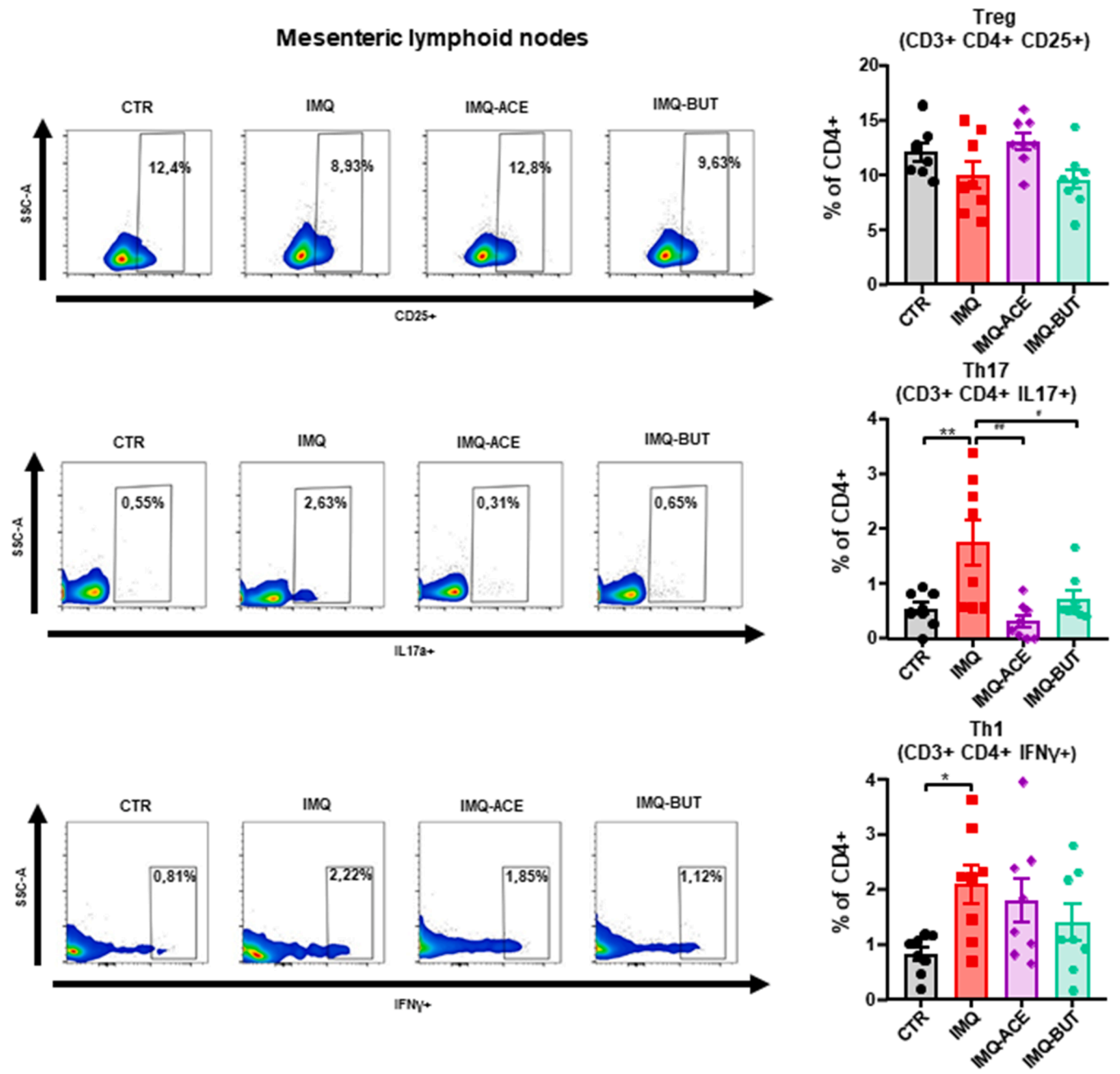

Fig. 6. Effects of SCFA treatments on lymphocyte populations in mesenteric lymph nodes of TLR7-induced lupus mice. Regulatory T cells (Treg), Th17, and Th1 cells measured by flow cytometry in control (CTR), imiquimod (IMQ), and IMQ-treated mice with acetate (ACE) or butyrate (BUT) groups. Data presented as % of parent and means ± SEM (n = 8). One-way ANOVA and Tukey's post hoc or Kruskal-Wallis with Dunn's multiple comparisons. *P < 0.05 and * *P < 0.01 vs. CTR; #P < 0.05 and ##P < 0.01 vs. untreated IMQ.

antigens to naïve CD4 + T lymphocytes, contributing to T cell priming. In alignment with this, we observed higher levels of *Cx3cr1* mRNA (approximately 3.6-fold increase) in MLNs from the IMQ group compared to the CTR mice, which were brought back to normal levels by acetate consumption, although not by butyrate consumption (Fig. S10A). Additionally, dendritic cells, apart from their role as antigen-presenting cells, release mediators that promote T cell polarization. IL-6 induces the proliferation of Th17 cells and suppresses Treg cells [54]. Our analysis of transcript levels in MLNs revealed that *Il-6* levels were approximately 5.9-fold higher in the IMQ group than in the CTR group, and acetate treatment reduced this elevation by about 45% (Fig. S10B). The activation of GPRs and inhibition of HDACs by SCFAs in immune cells have been previously documented [51]. We noted that acetate treatment upregulated *Gpr43* mRNA levels, while butyrate increased *Gpr41* expression and downregulated *Hdac3* (Fig. S10C). It has been described that sodium butyrate, acting as an HDAC inhibitor, regulates the balance between Th17 and Treg cells through the nuclear factor erythroid 2-related factor 2 (Nrf2)/heme oxygenase 1 (Hmox-1)/IL-6 receptor (IL-6R) pathway [55]. In line with Nrf2 activation, the mRNA levels of the downstream antioxidant enzymes *Hmox-1* and NAD(P)H:quinone oxidoreductase 1 (*Nqo1*) were increased by butyrate, leading to a decreased expression of the *Il-6r* (Fig. S10D) and resulting in a reduced Th17 polarization.

3.6. GPR43 blockade prevented the protective effects induced by acetate

To investigate the potential role of GPR43 in the effects of SCFAs, we utilized the GPR43 antagonist GLPG-0974. This drug counteracted the antihypertensive effects of acetate (Fig. 7A) and attenuated its ability to reduce heart hypertrophy (Fig. 7B), while having no impact on the effects of butyrate. Moreover, blocking GPR43 abolished the improvement of endothelium-dependent relaxation to acetylcholine induced by acetate, but not by butyrate treatment (Fig. 7C). The impaired relaxant response to acetylcholine induced by GLPG-0974 was mitigated in the presence of the NADPH oxidase inhibitor, VAS2870, or the Rho kinase inhibitor, Y27632 (Fig. 7C), suggesting that acetate reduced NADPH oxidase and Rho kinase activities through GPR43 activation. Indeed, GLPG-0974 increased NADPH oxidase activity in IMQ mice treated with acetate, bringing it to levels comparable to untreated IMQ mice (Fig. 7D). When aortic rings were incubated with an antibody to neutralize IL-17, the reduced endothelium-dependent relaxation to acetylcholine induced by GLPG-0974 in the presence of acetate was reversed (Fig. 7E), suggesting that acetate improved this relaxant response by reducing IL-17 production in the vascular wall. This finding was further supported by the increased Th17 infiltration observed in aortic rings from the GLPG-IMQ-acetate group (Fig. 7F). In contrast, GPR43 blockade had no effect on the protective responses induced by butyrate in IMQ mice, suggesting the involvement of GPR43-independent mechanisms.

3.7. SCFA treatments abolished the transfer of hypertensive phenotype induced by gut microbiota from IMQ mice in germ free mice

As anticipated, transferring the microbiota from donor IMQ group to recipient GF mice led to an increase in SBP by approximately 23 mmHg (Fig. 8A), induced left ventricular and kidney hypertrophy (Fig. 8B), impaired endothelium-dependent relaxation (Fig. 8C) through elevated NADPH oxidase activity (Fig. 8D), and increased aortic Th17 infiltration (Fig. 8E). This confirmed that the hypertensive phenotype can be transferred by the microbiota. In contrast, the signs of autoimmunity, such as plasma anti-ds-DNA (Fig. S11A), splenomegaly (Fig. S11B), hepatomegaly (Fig. S11C), and blood B cell content (Fig. S11D) were not transferred by microbiota inoculation for 3 weeks. Interestingly, both acetate and butyrate treatments abolished the transfer of the

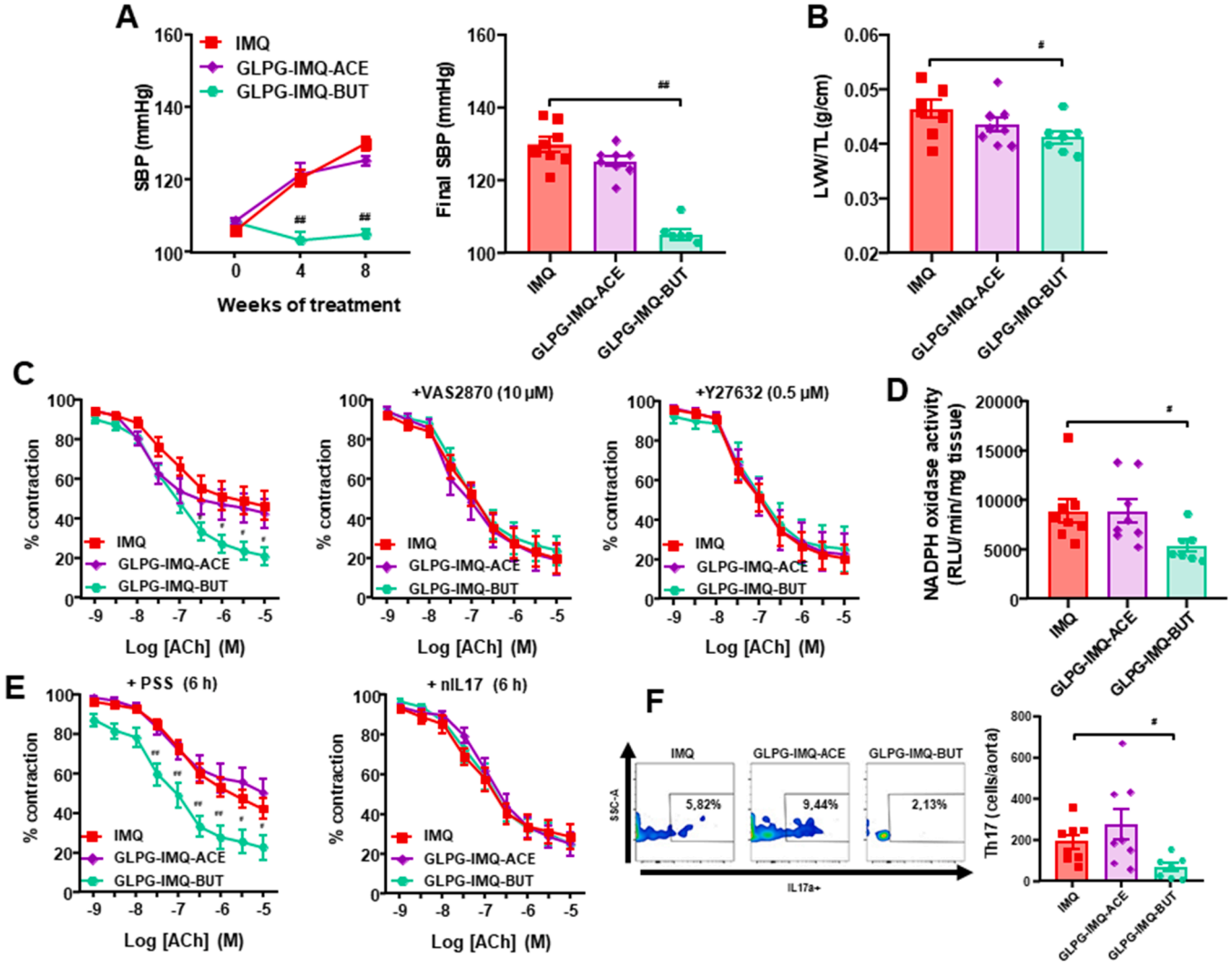

Fig. 7. Effects of pharmacological GPR43 blockade on SCFA treatments in TLR7-induced lupus mice. (A) Time-course and final systolic blood pressure (SBP), (B) left ventricular weight (LVW) normalized by tibia length (TL), (C) acetylcholine (Ach)-induced vascular relaxation, (D) aortic NADPH oxidase activity, (E) ACh-induced vascular relaxation after IL-17 neutralization, and (F) aortic immune cell infiltration. Groups: IMQ, IMQ treated with GPR43 blockade (GLPG) and acetate (ACE) or butyrate (BUT). Data presented as means ± SEM (n = 7–8). Two-way ANOVA with Sidak's multiple comparisons for SBP time-course and ACh concentration-response curves. One-way ANOVA and Tukey's post hoc or Kruskal-Wallis with Dunn's multiple comparisons for other variables. #P < 0.05 and ##P < 0.01 vs. untreated IMQ.

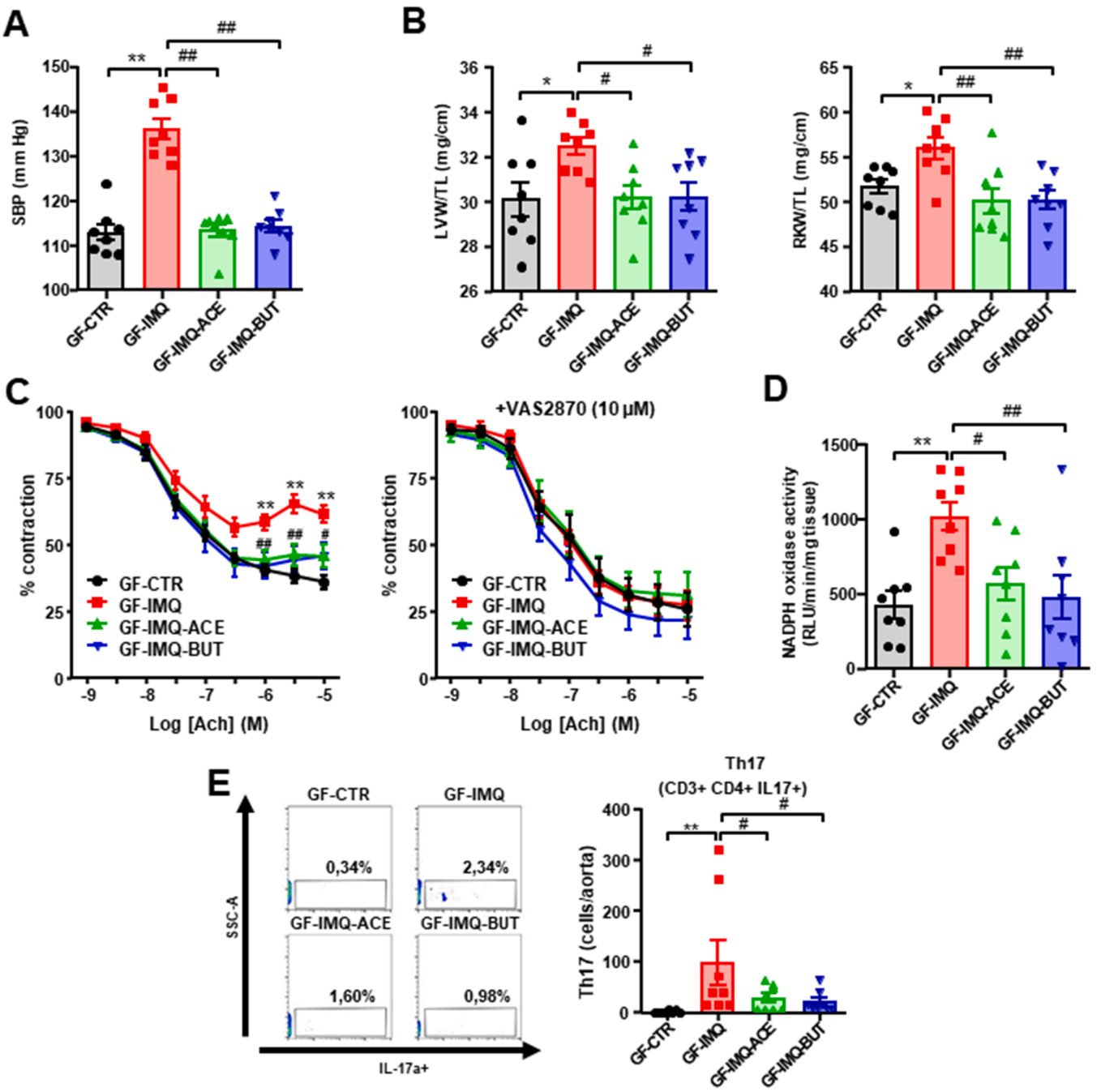

Fig. 8. Effects of SCFA treatments on hypertension transfer to germ-free mice from TLR7-induced lupus mice. (A) Systolic blood pressure (SBP) measured by tail-cuff plethysmography, (B) left ventricular weight (LVW) and right kidney weight (RKW) normalized by tibia length (TL), (C) acetylcholine (ACh)-induced vascular relaxation, (D) aortic NADPH oxidase activity, and (E) aortic immune cell infiltration. Groups: germ-free (GF) mice inoculated with control faeces (GF-CTR), IMQ faeces (GF-SLE), and IMQ faeces treated with acetate (GF-IMQ-ACE) or butyrate (GF-IMQ-BUT). Data presented as means ± SEM (n = 8). Two-way ANOVA with Sidak's multiple comparisons for SBP time-course and ACh concentration-response curves. One-way ANOVA and Tukey's post hoc or Kruskal-Wallis with Dunn's multiple comparisons for other variables. *P < 0.05 and * *P < 0.01 vs. GF-CTR; #P < 0.05 and ##P < 0.01 vs. GF-SLE.

hypertensive phenotype observed in mice inoculated with IMQ faeces. Furthermore, it was interesting to note that the hypertensive phenotype induced in GF mice by faecal inoculation from IMQ mice was associated with a higher proportion of Th17 cells in MLNs and blood, with no significant changes in Treg and Th1 cell abundance (Fig. S12). However, spleen showed no significant changes in the proportion of Th17, Treg, and Th1 cells after microbiota inoculation. Acetate treatment reduced Th17 content in MLNs and blood, whereas butyrate increased MLNs and circulating Treg cells while reducing Th17 cells in MLNs. Overall, our data demonstrated that SCFAs treatments restored the Th17/Treg balance in GF mice inoculated with faeces from IMQ mice, reducing vascular Th17 infiltration, which led to improved endothelial dysfunction and BP normalization.

4. Discussion

In this study, we have demonstrated the significance of SCFAs derived from gut microbiota in preventing cardiovascular complications associated with lupus induced by TLR7 activation. Specifically, we have identified GPR43-dependent immune modulation in gut secondary

lymph nodes induced by acetate, which is linked to the improvement of endothelial dysfunction and reduction of BP. On the other hand, the preventive effect of butyrate in vascular dysfunction seems to be related to the rebalancing of Th17/Tregs polarization through GPR41 activation and/or HDAC inhibition. However, neither butyrate nor acetate were able to prevent the development of systemic autoimmunity. Furthermore, we have found that the chronic consumption of insoluble (RS) or soluble (ITF) fibers, acting as dietary sources of SCFAs, exerted similar cardiovascular protective effects as acetate or butyrate supplementation alone. Moreover, we have demonstrated through faecal inoculation of dysbiotic microbiota from donor IMQ mice to recipient GF mice that gut microbiota plays a key role in the generation of endothelial dysfunction and high BP, mediated by the increase in Th17 cells in MLNs, blood, and vascular wall. SCFAs treatment effectively abolished the transfer of this hypertensive phenotype.

Gut leakiness was found to be TLR7 dependent, as demonstrated in studies with TLR7 knockout mice [13] and in autoimmune conditions induced by TLR7 activation [12,56]. However, the physiological function of TLR7 in the gut, particularly on the gut epithelium, remains poorly understood. In our current study, we have observed that gut leakiness is involved in Th17 differentiation in MLNs, as it facilitates the accumulation of antigen-presenting cells, activates T CD4 + naïve cells, and increases IL-6 production. This supports the notion that gut integrity plays a critical role in gut immune modulation. We have demonstrated that acetate, which reduces colonic leakiness, also inhibits the accumulation of CX3CR1 + cells in MLNs and reduces IL-6-driven Th17 polarization. Moreover, we found that the reduction in Th17 proportion in MLNs induced by acetate was abolished by the blockade of GPR43, highlighting the key role of GPR43 activation in the immune modulatory effects of acetate. In contrast, butyrate was unable to improve gut leakiness or reduce CX3CR1 + cells and IL-6 levels in MLNs. However, butyrate was effective in reducing IL-6 receptor expression, thereby preventing Th17 polarization. This effect seems to be mediated by the reduction in *Hdac3* mRNA levels, leading to the activation of the Nrf2/HO-1 pathway in MLNs, as described previously [55].

Endothelial dysfunction plays a key role in the development of hypertension, where decreased nitric oxide (NO) bioavailability connects oxidative stress to endothelial dysfunction and elevated BP. Both innate and adaptive immune responses contribute to the generation of ROS and inflammatory changes in the kidneys, blood vessels, and brain during hypertension [57]. In the context of SLE mice, dysfunctional communication between the immune system and vascular wall is involved in endothelial dysfunction [58,59]. Our current findings support the critical role of IL-17 derived from Th17 cells in vascular wall dysfunction and elevated BP observed in autoimmunity induced by TLR7 activation [10,12,14]. Importantly, SCFAs treatments and fiber consumption reduced Th17 infiltration in the vascular wall, resulting in improved vascular NADPH oxidase-driven ROS production and restoration of impaired endothelium-dependent relaxation. ROS production by vascular NADPH oxidase is considered crucial in endothelial dysfunction, as demonstrated by the beneficial effects of the selective NADPH oxidase inhibitor VAS2870, which improved aortic endothelium-dependent relaxation to acetylcholine. NADPH oxidase activity can be modulated by local and circulating cytokines [60,61]. IL-17, a pro-inflammatory cytokine, has been shown to induce Rho-kinase-mediated endothelial dysfunction in the vasculature, likely due to increased ROS generation through NADPH oxidase activation [49,62]. Our results in this SLE model suggest that the IL-17-Rho-kinase pathway is significantly influenced by SCFAs. This is supported by the restoration of acetylcholine relaxation observed with SCFAs or fiber treatments, similar to the effects of the Rho-kinase inhibitor Y27632. Additionally, neutralizing IL-17 in aortic rings from IMQ mice also improved endothelial dysfunction. Interestingly, the reduction in aortic Th17 infiltration and improvement of endothelium-dependent relaxation induced by acetate were abolished by GLPG-0974, confirming the crucial role of GPR43 activation in its vasculo-protective effects. An important limitation of our study is the lack of confirmation of these results in GPR43$^{-/-}$ mice.

Activation of TLR-4 in blood vessels by bacterial products such as LPS leads to increased NADPH oxidase-dependent O_2^- production and inflammation [52]. In the case of IMQ mice, plasma endotoxin levels were elevated, and interventions aimed at reducing endotoxemia normalized vascular TLR-4 expression, thereby improving both vascular oxidative stress and inflammation [38,58]. Our study observed heightened plasma levels of LPS in IMQ mice, which correlated with decreased colonic integrity. Notably, administration of acetate effectively reduced endotoxemia and improved endothelial dysfunction. This suggests that the decrease in aortic TLR-4 activation by LPS also contributed to the attenuation of vascular oxidative stress induced by acetate.

Previous reports have demonstrated that preventing autoimmunity through anti-CD20 therapy [63] or depleting plasma cells with bortezomib [25] guards against the development of SLE-induced hypertension. As expected, we noted elevated B cell populations in the spleens of IMQ mice compared to the CTR group. However, neither acetate nor butyrate treatments reduced B cell generation or plasma anti-ds-DNA levels, indicating that B cells and autoantibodies are not implicated in the BP regulation induced by SCFAs. Moreover, faecal microbiota transplantation from IMQ mice to GF mice did not elevate the proportion of B cells in blood, yet it impaired endothelial function and heightened BP. Interestingly, SCFA treatments managed to ameliorate these cardiovascular abnormalities. Among them, only a diet rich in resistant starch (RS), which augmented the production of acetate, butyrate, and propionate by gut bacteria, thwarted signs of autoimmunity by modulating the TLR7-IFN axis, a vital factor in human SLE [9].

In summary, our study demonstrates that SCFA interventions partially thwarted hypertension development and mitigated cardiac hypertrophy and endothelial dysfunction in TLR7-activated SLE-induced mice. These effects correlated with enhanced gut integrity, reduced endotoxemia, and decreased Th17 infiltration in the vascular wall. Additionally, dietary fiber interventions, which bolstered SCFAs production by gut microbiota in IMQ mice, rebalanced the gut-immune system, counteracted endothelial dysfunction, and provided protection against hypertension. Given that individuals with SLE have reported lower fiber intake compared to healthy individuals [64,65], and considering the observed inverse correlation between dietary fiber intake and active SLE risk [66], our findings suggest a potential role for RS-rich fiber treatment in preventing autoimmunity and SLE-related cardiovascular complications. This is especially relevant for patients exhibiting SLE phenotypes associated with increased TLR7 signaling, elevated IgD-CD27- double-negative B cells in peripheral blood [67], and excessive accumulation of extrafollicular helper T cells [68].

Importantly, dietary interventions such as fiber-rich diets or SCFA treatments may provide a more targeted and potentially safer approach compared to broad-spectrum antibiotics, which can lead to side effects ranging from diarrheal events, disruption of the native microbiota, to more serious concerns like antibiotic resistance and systemic toxicities [12]. However, it is vital to exercise caution when extrapolating our findings to humans due to documented differences between animal and human microbiota features.

CRediT authorship contribution statement

Conceptualization, J.D. and M.R.; Methodology, I.R.-V., N.d.l.V., A. M.B. and M.G.-G.; Software, J.M. and I.R.-V.; Validation, J.M. and I.R.-V.; Formal analysis, J.D. and M.R.; Investigation, J.M., C.G.-C., S.M., I. R.-V., N.d.l.V., A.M.B., M.G.-G., M.S., P.R., E.G.-H., M.T. and M.R; Resources, J.D. and M.R.; Data curation, J.D.; Writing – original draft, J.D.; Writing–review & editing, J.D. and M.R.; Visualization, J.M., C.G.-C., S. M. and I.R.-V.; Supervision, J.D. and M.R.; Project administration, J.D.; Funding acquisition, J.D. and M.R.

Declaration of Competing Interest

The authors declare that they have no known competing financial interests or personal relationships that could have appeared to influence the work reported in this paper.

Data availability

Data will be made available on request.

Acknowledgments

This work was supported by Grants from Ministry of Science and Innovation of Spain (MCIN) (Ref. PID2020-116347RB-I00 funded by MCIN/AEI/ 10.13039/501100011033) co-funded by the European Regional Development Fund FEDER, Consejería de Universidad, Investigación e Innovación de la Junta de Andalucía (Ref. CTS 164, P20_00193, and A-CTS-318-UGR20) with funds from the European Union, and by the Instituto de Salud Carlos III (PI22/01046, CIBER-CV). IR-V is postdoctoral funded by MINECO (FJC2021-048099-I). J.M. is a predoctoral fellow of MINECO (FPU18/02561), and C.G.-C. and S.M. are predoctoral fellow of Junta de Andalucía. The cost of this publication was paid in part with funds from the European Union (Fondo Europeo de Desarrollo Regional, FEDER, "FEDER una manera de hacer Europa"). The authors thank N. Rodríguez and V. Plaza for technical assistance.

Appendix A. Supporting information

Supplementary data associated with this article can be found in the online version at doi:10.1016/j.phrs.2023.106997.

References

[1] S. Manzi, E.N. Meilahn, J.E. Rairie, C.G. Conte, T.A. Medsger, L. Jansen-Mcwilliams, R.B. D'agostino, L.H. Kuller, Age-specific Incidence Rates of Myocardial Infarction and Angina in Women with Systemic Lupus Erythematosus: Comparison with the Framingham Study, 1997. ⟨https://academic.oup.com/aje/article-abstract/145/5/408/120887⟩.

[2] C.M. Bartels, K.A. Buhr, J.W. Goldberg, C.L. Bell, M. Visekruna, S. Nekkanti, R. T. Greenlee, Mortality and cardiovascular burden of systemic lupus erythematosus in a US population-based cohort, J. Rheumatol. 41 (2014) 680–687, https://doi.org/10.3899/jrheum.130874.

[3] M. Zhao, R. Feng, V.P. Werth, K.J. Williams, State of current management of the heightened risk for atherosclerotic cardiovascular events in an established cohort of patients with lupus erythematosus, Lupus Sci. Med. 10 (2023), https://doi.org/10.1136/lupus-2023-000908.

[4] Y. Wu, W. Tang, J. Zuo, Toll-like receptors: potential targets for lupus treatment, Acta Pharmacol. Sin. 36 (2015) 1395–1407, https://doi.org/10.1038/aps.2015.91.

[5] M. Weidenbusch, O.P. Kulkarni, H.-J. Anders, The innate immune system in human systemic lupus erythematosus, Clin. Sci. (Lond.). 131 (2017) 625–634, https://doi.org/10.1042/CS20160415.

[6] M. Yokogawa, M. Takaishi, K. Nakajima, R. Kamijima, C. Fujimoto, S. Kataoka, Y. Terada, S. Sano, Epicutaneous application of toll-like receptor 7 agonists leads to systemic autoimmunity in wild-type mice: a new model of systemic Lupus erythematosus, Arthritis Rheumatol. 66 (2014) 694–706, https://doi.org/10.1002/art.38298.

[7] T. Celhar, A.-M. Fairhurst, Modelling clinical systemic lupus erythematosus: similarities, differences and success stories, Rheumatology 56 (2017) i88–i99, https://doi.org/10.1093/rheumatology/kew400.

[8] G.J. Brown, P.F. Cañete, H. Wang, A. Medhavy, J. Bones, J.A. Roco, Y. He, Y. Qin, J. Cappello, J.I. Ellyard, K. Bassett, Q. Shen, G. Burgio, Y. Zhang, C. Turnbull, X. Meng, P. Wu, E. Cho, L.A. Miosge, T.D. Andrews, M.A. Field, D. Tvorogov, A. F. Lopez, J.J. Babon, C.A. López, Á. Gónzalez-Murillo, D.C. Garulo, V. Pascual, T. Levy, E.J. Mallack, D.G. Calame, T. Lotze, J.R. Lupski, H. Ding, T.R. Ullah, G. D. Walters, M.E. Koina, M.C. Cook, N. Shen, C. de Lucas Collantes, B. Corry, M. P. Gantier, V. Athanasopoulos, C.G. Vinuesa, TLR7 gain-of-function genetic variation causes human lupus, Nature 605 (2022) 349–356, https://doi.org/10.1038/s41586-022-04642-z.

[9] M.K. Crow, Type I interferon in the pathogenesis of lupus, J. Immunol. 192 (2014) 5459–5468, https://doi.org/10.4049/jimmunol.1002795.

[10] I. Robles-Vera, N.D.La Visitación, M. Toral, M. Sánchez, M. Gómez-Guzmán, F. O'valle, R. Jiménez, J. Duarte, M. Romero, Toll-like receptor 7-driven lupus autoimmunity induces hypertension and vascular alterations in mice, J. Hypertens. 38 (2020) 1322–1335, https://doi.org/10.1097/HJH.0000000000002368.

[11] A.S. Elshikha, X.Y. Teng, N. Kanda, W. Li, S.-C. Choi, G. Abboud, M. Terrell, K. Fredenburg, L. Morel, TLR7 activation accelerates cardiovascular pathology in a mouse model of lupus, Front. Immunol. 13 (2022), 914468, https://doi.org/10.3389/fimmu.2022.914468.

[12] N. de la Visitación, I. Robles-Vera, J. Moleón, C. González-Correa, N. Aguilera-Sánchez, M. Toral, M. Gómez-Guzmán, M. Sánchez, R. Jiménez, N. Martin-Morales, F. O'Valle, M. Romero, J. Duarte, Gut microbiota has a crucial role in the development of hypertension and vascular dysfunction in toll-like receptor 7-driven lupus autoimmunity, Antioxidants 10 (2021), https://doi.org/10.3390/antiox10091426.

[13] D.F. Zegarra-Ruiz, A. El Beidaq, A.J. Iniguez, M. Lubrano Di Ricco, S. Manfredo Vieira, W.E. Ruff, D. Mubiru, R.L. Fine, J. Sterpka, T.M. Greiling, C. Dehner, M. A. Kriegel, A diet-sensitive commensal lactobacillus strain mediates TLR7-dependent systemic autoimmunity, Cell Host Microbe 25 (2019) 113–127.e6, https://doi.org/10.1016/j.chom.2018.11.009.

[14] N. de la Visitación, I. Robles-Vera, J. Moleón-Moya, M. Sánchez, R. Jiménez, M. Gómez-Guzmán, C. González-Correa, M. Olivares, M. Toral, M. Romero, J. Duarte, Probiotics prevent hypertension in a murine model of systemic lupus erythematosus induced by toll-like receptor 7 activation, Nutrients 13 (2021), https://doi.org/10.3390/nu13082669.

[15] P.V. Chang, L. Hao, S. Offermanns, R. Medzhitov, The microbial metabolite butyrate regulates intestinal macrophage function via histone deacetylase inhibition, Proc. Natl. Acad. Sci. U. S. A. 111 (2014) 2247–2252, https://doi.org/10.1073/pnas.1322269111.

[16] F.Z. Marques, E. Nelson, P.-Y. Chu, D. Horlock, A. Fiedler, M. Ziemann, J.K. Tan, S. Kuruppu, N.W. Rajapakse, A. El-Osta, C.R. Mackay, D.M. Kaye, High-fiber diet and acetate supplementation change the gut microbiota and prevent the development of hypertension and heart failure in hypertensive mice, Circulation 135 (2017) 964–977, https://doi.org/10.1161/CIRCULATIONAHA.116.024545.

[17] L. Wang, Q. Zhu, A. Lu, X. Liu, L. Zhang, C. Xu, X. Liu, H. Li, T. Yang, Sodium butyrate suppresses angiotensin II-induced hypertension by inhibition of renal (pro)renin receptor and intrarenal renin-angiotensin system, J. Hypertens. 35 (2017) 1899–1908, https://doi.org/10.1097/HJH.0000000000001378.

[18] S. Kim, R. Goel, A. Kumar, Y. Qi, G. Lobaton, K. Hosaka, M. Mohammed, E. M. Handberg, E.M. Richards, C.J. Pepine, M.K. Raizada, Imbalance of gut microbiome and intestinal epithelial barrier dysfunction in patients with high blood pressure, Clin. Sci. (2018), https://doi.org/10.1042/CS20180087.

[19] H. Bartolomaeus, A. Balogh, M. Yakoub, S. Homann, L. Markó, S. Höges, D. Tsvetkov, A. Krannich, S. Wundersitz, E.G. Avery, N. Haase, K. Kräker, L. Hering, M. Maase, K. Kusche-Vihrog, M. Grandoch, J. Fielitz, S. Kempa, M. Gollasch, Z. Zhumadilov, S. Kozhakhmetov, A. Kushugulova, K.-U. Eckardt, R. Dechend, L.C. Rump, S.K. Forslund, D.N. Müller, J. Stegbauer, N. Wilck, Short-chain fatty acid propionate protects from hypertensive cardiovascular damage, Circulation 139 (2019) 1407–1421, https://doi.org/10.1161/CIRCULATIONAHA.118.036652.

[20] I. Robles-Vera, N. de la Visitación, M. Toral, M. Sánchez, M. Romero, M. Gómez-Guzmán, T. Yang, J.L. Izquierdo-García, E. Guerra-Hernández, J. Ruiz-Cabello, M. K. Raizada, F. Pérez-Vizcaíno, R. Jiménez, J. Duarte, Probiotic Bifidobacterium breve prevents DOCA-salt hypertension, FASEB J. . Publ. Fed. Am. Soc. Exp. Biol. 34 (2020) 13626–13640, https://doi.org/10.1096/fj.202001532R.

[21] I. Robles-Vera, M. Toral, N. de la Visitación, M. Sánchez, M. Gómez-Guzmán, M. Romero, T. Yang, J.L. Izquierdo-Garcia, R. Jiménez, J. Ruiz-Cabello, E. Guerra-Hernández, M.K. Raizada, F. Pérez-Vizcaíno, J. Duarte, Probiotics prevent dysbiosis and the rise in blood pressure in genetic hypertension: role of short-chain fatty acids, Mol. Nutr. Food Res. 64 (2020), e1900616, https://doi.org/10.1002/mnfr.201900616.

[22] D.M. Kaye, W.A. Shihata, H.A. Jama, K. Tsyganov, M. Ziemann, H. Kiriazis, D. Horlock, A. Vijay, B. Giam, A. Vinh, C. Johnson, A. Fiedler, D. Donner, M. Snelson, M.T. Coughlan, S. Phillips, X.-J. Du, A. El-Osta, G. Drummond, G. W. Lambert, T.D. Spector, A.M. Valdes, C.R. Mackay, F.Z. Marques, Deficiency of prebiotic fiber and insufficient signaling through gut metabolite-sensing receptors leads to cardiovascular disease, Circulation 141 (2020) 1393–1403, https://doi.org/10.1161/CIRCULATIONAHA.119.043081.

[23] J. Jin, L. Gao, X. Zou, Y. Zhang, Z. Zheng, X. Zhang, J. Li, Z. Tian, X. Wang, J. Gu, C. Zhang, T. Wu, Z. Wang, Q. Zhang, Gut dysbiosis promotes preeclampsia by regulating macrophages and trophoblasts, Circ. Res. 131 (2022) 492–506, https://doi.org/10.1161/CIRCRESAHA.122.320771.

[24] H.A. Jama, D. Rhys-Jones, M. Nakai, C.K. Yao, R.E. Climie, Y. Sata, D. Anderson, D. J. Creek, G.A. Head, D.M. Kaye, C.R. Mackay, J. Muir, F.Z. Marques, Prebiotic intervention with HAMSAB in untreated essential hypertensive patients assessed in a phase II randomized trial, Nat. Cardiovasc. Res. 2 (2023) 35–43, https://doi.org/10.1038/s44161-022-00197-4.

[25] E.B. Taylor, M.T. Barati, D.W. Powell, H.R. Turbeville, M.J. Ryan, Plasma cell depletion attenuates hypertension in an experimental model of autoimmune disease, Hypertensions 71 (2018) 719–728, https://doi.org/10.1161/HYPERTENSIONAHA.117.10473.

[26] J. Moleón, C. González-Correa, I. Robles-Vera, S. Miñano, N. de la Visitación, A. M. Barranco, N. Martín-Morales, F. O'Valle, L. Mayo-Martínez, A. García, M. Toral, R. Jiménez, M. Romero, J. Duarte, Targeting the gut microbiota with dietary fibers: a novel approach to prevent the development cardiovascular complications linked to systemic lupus erythematosus in a preclinical study, Gut Microbes 15 (2023), 2247053, https://doi.org/10.1080/19490976.2023.2247053.

[27] M.A.R. Vinolo, H.G. Rodrigues, R.T. Nachbar, R. Curi, Regulation of inflammation by short chain fatty acids, Nutrients 3 (2011) 858–876, https://doi.org/10.3390/nu3100858.

[28] I. Robles-Vera, M. Toral, N. de la Visitación, N. Aguilera-Sánchez, J.M. Redondo, J. Duarte, Protective effects of short-chain fatty acids on endothelial dysfunction

induced by angiotensin II, Front. Physiol. 11 (2020), 277, https://doi.org/10.3389/fphys.2020.00277.
[29] A.J. Brown, S.M. Goldsworthy, A.A. Barnes, M.M. Eilert, L. Tcheang, D. Daniels, A. I. Muir, M.J. Wigglesworth, I. Kinghorn, N.J. Fraser, N.B. Pike, J.C. Strum, K. M. Steplewski, P.R. Murdock, J.C. Holder, F.H. Marshall, P.G. Szekeres, S. Wilson, D.M. Ignar, S.M. Foord, A. Wise, S.J. Dowell, The Orphan G protein-coupled receptors GPR41 and GPR43 are activated by propionate and other short chain carboxylic acids, J. Biol. Chem. 278 (2003) 11312–11319, https://doi.org/10.1074/jbc.M211609200.
[30] Y.-H. Hong, Y. Nishimura, D. Hishikawa, H. Tsuzuki, H. Miyahara, C. Gotoh, K.-C. Choi, D.D. Feng, C. Chen, H.-G. Lee, K. Katoh, S.-G. Roh, S. Sasaki, Acetate and propionate short chain fatty acids stimulate adipogenesis via GPCR43, Endocrinology 146 (2005) 5092–5099, https://doi.org/10.1210/en.2005-0545.
[31] X. Zheng, T. Zhou, X.-A. Wang, X. Tong, J. Ding, Histone deacetylases and atherosclerosis, Atherosclerosis 240 (2015) 355–366, https://doi.org/10.1016/j.atherosclerosis.2014.12.048.
[32] F.Z. Marques, H.A. Jama, K. Tsyganov, P.A. Gill, D. Rhys-Jones, R.R. Muralitharan, J. Muir, A. Holmes, C.R. Mackay, Guidelines for transparency on gut microbiome studies in essential and experimental hypertension, Hypertensions 74 (2019) 1279–1293, https://doi.org/10.1161/HYPERTENSIONAHA.119.13079.
[33] N. Percie du Sert, V. Hurst, A. Ahluwalia, S. Alam, M.T. Avey, M. Baker, W. J. Browne, A. Clark, I.C. Cuthill, U. Dirnagl, M. Emerson, P. Garner, S.T. Holgate, D.W. Howells, N.A. Karp, S.E. Lazic, K. Lidster, C.J. MacCallum, M. Macleod, E. J. Pearl, O.H. Petersen, F. Rawle, P. Reynolds, K. Rooney, E.S. Sena, S. D. Silberberg, T. Steckler, H. Würbel, The ARRIVE guidelines 2.0: Updated guidelines for reporting animal research, Br. J. Pharmacol. 177 (2020) 3617–3624, https://doi.org/10.1111/bph.15193.
[34] M. Souyris, J.E. Mejía, J. Chaumeil, J.-C. Guéry, Female predisposition to TLR7-driven autoimmunity: gene dosage and the escape from X chromosome inactivation, Semin. Immunopathol. 41 (2019) 153–164, https://doi.org/10.1007/s00281-018-0712-y.
[35] E. Catry, L.B. Bindels, A. Tailleux, S. Lestavel, A.M. Neyrinck, J.-F. Goossens, I. Lobysheva, H. Plovier, A. Essaghir, J.-B. Demoulin, C. Bouzin, B.D. Pachikian, P. D. Cani, B. Staels, C. Dessy, N.M. Delzenne, Targeting the gut microbiota with inulin-type fructans: preclinical demonstration of a novel approach in the management of endothelial dysfunction, Gut 67 (2018) 271–283, https://doi.org/10.1136/gutjnl-2016-313316.
[36] F. Namour, R. Galien, T. Van Kaem, A. Van der Aa, F. Vanhoutte, J. Beetens, G. Van't Klooster, Safety, pharmacokinetics and pharmacodynamics of GLPG0974, a potent and selective FFA2 antagonist, in healthy male subjects, Br. J. Clin. Pharmacol. 82 (2016) 139–148, https://doi.org/10.1111/bcp.12900.
[37] J.J. Yang, M.T. Pham, A.R. Rahim, T.-H. Chuang, M.-F. Hsieh, C.-M. Huang, Mouse abdominal fat depots reduced by butyric acid-producing leuconostoc mesenteroides, Microorganisms 8 (2020), https://doi.org/10.3390/microorganisms8081180.
[38] N. de la Visitación, I. Robles-Vera, M. Toral, M. Gómez-Guzmán, M. Sánchez, J. Moleón, C. González-Correa, N. Martín-Morales, F. O'Valle, R. Jiménez, M. Romero, J. Duarte, Gut microbiota contributes to the development of hypertension in a genetic mouse model of systemic lupus erythematosus, Br. J. Pharmacol. 178 (2021) 3708–3729, https://doi.org/10.1111/bph.15512.
[39] R. Lavin, N. DiBenedetto, V. Yeliseyev, M. Delaney, L. Bry, Gnotobiotic and conventional mouse systems to support microbiota based studies, Curr. Protoc. Immunol. 121 (2018), e48, https://doi.org/10.1002/cpim.48.
[40] V.S. Dole, K.S. Henderson, R.D. Fister, M.T. Pietrowski, G. Maldonado, C. B. Clifford, Pathogenicity and genetic variation of 3 strains of Corynebacterium bovis in immunodeficient mice, J. Am. Assoc. Lab. Anim. Sci. 52 (2013) 458–466.
[41] J.G. Caporaso, C.L. Lauber, W.A. Walters, D. Berg-Lyons, C.A. Lozupone, P. J. Turnbaugh, N. Fierer, R. Knight, Global patterns of 16S rRNA diversity at a depth of millions of sequences per sample, Proc. Natl. Acad. Sci. U. S. A. 108 (Suppl) (2011) 4516–4522, https://doi.org/10.1073/pnas.1000080107.
[42] H.-W. Zhou, D.-F. Li, N.F.-Y. Tam, X.-T. Jiang, H. Zhang, H.-F. Sheng, J. Qin, X. Liu, F. Zou, BIPES, a cost-effective high-throughput method for assessing microbial diversity, ISME J. 5 (2011) 741–749, https://doi.org/10.1038/ismej.2010.160.
[43] Z. Liu, H.-Y. Liu, H. Zhou, Q. Zhan, W. Lai, Q. Zeng, H. Ren, D. Xu, Moderate-intensity exercise affects gut microbiome composition and influences cardiac function in myocardial infarction mice, Front. Microbiol. 8 (2017), 1687, https://doi.org/10.3389/fmicb.2017.01687.
[44] R.C. Edgar, H. Flyvbjerg, Error filtering, pair assembly and error correction for next-generation sequencing reads, Bioinformatics 31 (2015) 3476–3482, https://doi.org/10.1093/bioinformatics/btv401.
[45] Q. Zeng, D. Li, Y. He, Y. Li, Z. Yang, X. Zhao, Y. Liu, Y. Wang, J. Sun, X. Feng, F. Wang, J. Chen, Y. Zheng, Y. Yang, X. Sun, X. Xu, D. Wang, T. Kenney, Y. Jiang, H. Gu, Y. Li, K. Zhou, S. Li, W. Dai, Discrepant gut microbiota markers for the classification of obesity-related metabolic abnormalities, Sci. Rep. 9 (2019), 13424, https://doi.org/10.1038/s41598-019-49462-w.
[46] W.-J. Xia, M.-L. Xu, X.-J. Yu, M.-M. Du, X.-H. Li, T. Yang, L. Li, Y. Li, K.B. Kang, Q. Su, J.-X. Xu, X.-L. Shi, X.-M. Wang, H.-B. Li, Y.-M. Kang, Antihypertensive effects of exercise involve reshaping of gut microbiota and improvement of gut-brain axis in spontaneously hypertensive rat, Gut Microbes 13 (2021) 1–24, https://doi.org/10.1080/19490976.2020.1854642.
[47] E.D. Frohlich, C. Apstein, A.V. Chobanian, R.B. Devereux, H.P. Dustan, V. Dzau, F. Fauad-Tarazi, M.J. Horan, M. Marcus, B. Massie, The heart in hypertension, N. Engl. J. Med. 327 (1992) 998–1008, https://doi.org/10.1056/NEJM199210013271406.
[48] C.E. MacKay, Y. Shaifta, V.V. Snetkov, A.A. Francois, J.P.T. Ward, G.A. Knock, ROS-dependent activation of RhoA/Rho-kinase in pulmonary artery: Role of Src-family kinases and ARHGEF1, Free Radic. Biol. Med. 110 (2017) 316–331, https://doi.org/10.1016/j.freeradbiomed.2017.06.022.
[49] E. Pietrowski, B. Bender, J. Huppert, R. White, H.J. Luhmann, C.R.W. Kuhlmann, Pro-inflammatory effects of interleukin-17A on vascular smooth muscle cells involve NAD(P)H- oxidase derived reactive oxygen species, J. Vasc. Res. 48 (2011) 52–58, https://doi.org/10.1159/000317400.
[50] A. Ritzhaupt, I.S. Wood, A. Ellis, K.B. Hosie, S.P. Shirazi-Beechey, Identification and characterization of a monocarboxylate transporter (MCT1) in pig and human colon: its potential to transport L-lactate as well as butyrate. J. Physiol. 513 (Pt 3) (1998) 719–732, https://doi.org/10.1111/j.1469-7793.1998.719ba.x.
[51] D. Parada Venegas, M.K. De la Fuente, G. Landskron, M.J. González, R. Quera, G. Dijkstra, H.J.M. Harmsen, K.N. Faber, M.A. Hermoso, Corrigendum: short chain fatty acids (SCFAs)-mediated gut epithelial and immune regulation and its relevance for inflammatory bowel diseases, Front. Immunol. 10 (2019), 1486, https://doi.org/10.3389/fimmu.2019.01486.
[52] C.F. Liang, J.T. Liu, Y. Wang, A. Xu, P.M. Vanhoutte, Toll-like receptor 4 mutation protects obese mice against endothelial dysfunction by decreasing NADPH oxidase isoforms 1 and 4, Arterioscler, Thromb. Vasc. Biol. 33 (2013) 777–784, https://doi.org/10.1161/ATVBAHA.112.301087.
[53] J.H. Niess, S. Brand, X. Gu, L. Landsman, S. Jung, B.A. McCormick, J.M. Vyas, M. Boes, H.L. Ploegh, J.G. Fox, D.R. Littman, H.-C. Reinecker, CX3CR1-mediated dendritic cell access to the intestinal lumen and bacterial clearance, Science 307 (2005) 254–258, https://doi.org/10.1126/science.1102901.
[54] A. Kimura, T. Kishimoto, IL-6: regulator of Treg/Th17 balance, Eur. J. Immunol. 40 (2010) 1830–1835, https://doi.org/10.1002/eji.201040391.
[55] X. Chen, W. Su, T. Wan, J. Yu, W. Zhu, F. Tang, G. Liu, N. Olsen, D. Liang, S. G. Zheng, Sodium butyrate regulates Th17/Treg cell balance to ameliorate uveitis via the Nrf2/HO-1 pathway, Biochem. Pharmacol. 142 (2017) 111–119, https://doi.org/10.1016/j.bcp.2017.06.136.
[56] C. González-Correa, J. Moleón, S. Miñano, N. de la Visitación, I. Robles-Vera, M. Gómez-Guzmán, R. Jiménez, M. Romero, J. Duarte, Trimethylamine N-oxide promotes autoimmunity and a loss of vascular function in toll-like receptor 7-driven lupus mice, Antioxidants 11 (2021), https://doi.org/10.3390/antiox11010084.
[57] R.M. Zhang, K.P. McNerney, A.E. Riek, C. Bernal-Mizrachi, Immunity and hypertension, Acta Physiol. 231 (2021), e13487, https://doi.org/10.1111/apha.13487.
[58] M. Toral, I. Robles-Vera, M. Romero, N. de la Visitacion, M. Sanchez, F. O'Valle, A. Rodriguez-Nogales, J. Galvez, J. Duarte, R. Jimenez, Lactobacillus fermentum CECT5716: a novel alternative for the prevention of vascular disorders in a mouse model of systemic lupus erythematosus, FASEB J. . Publ. Fed. Am. Soc. Exp. Biol. 33 (2019) 10005–10018, https://doi.org/10.1096/fj.201900545RR.
[59] M. Romero, M. Toral, I. Robles-Vera, M. Sanchez, R. Jimenez, F. O'Valle, A. Rodriguez-Nogales, F. Perez-Vizcaino, J. Galvez, J. Duarte, Activation of peroxisome proliferator activator receptor beta/delta improves endothelial dysfunction and protects kidney in murine lupus, Hypertensions 69 (2017) 641–650, https://doi.org/10.1161/HYPERTENSIONAHA.116.08655.
[60] M.J. Ryan, An update on immune system activation in the pathogenesis of hypertension, Hypertension 62 (2013) 226–230, https://doi.org/10.1161/HYPERTENSIONAHA.113.00603.
[61] V.R. Kelley, R.P. Wuthrich, Cytokines in the pathogenesis of systemic lupus erythematosus, Semin. Nephrol. 19 (1999) 57–66.
[62] H. Nguyen, V.L. Chiasson, P. Chatterjee, S.E. Kopriva, K.J. Young, B.M. Mitchell, Interleukin-17 causes Rho-kinase-mediated endothelial dysfunction and hypertension, Cardiovasc. Res. 97 (2013) 696–704, https://doi.org/10.1093/cvr/cvs422.
[63] K.W. Mathis, K. Wallace, E.R. Flynn, C. Maric-Bilkan, B. LaMarca, M.J. Ryan, Preventing autoimmunity protects against the development of hypertension and renal injury, Hypertensions 64 (2014) 792–800, https://doi.org/10.1161/HYPERTENSIONAHA.114.04006.
[64] A.-L. Schäfer, A. Eichhorst, C. Hentze, A.N. Kraemer, A. Amend, D.T.L. Sprenger, C. Fluhr, S. Finzel, C. Daniel, U. Salzer, M. Rizzi, R.E. Voll, N. Chevalier, Low dietary fiber intake links development of obesity and lupus pathogenesis, Front. Immunol. 12 (2021), 696810, https://doi.org/10.3389/fimmu.2021.696810.
[65] A.-C. Elkan, C. Anania, T. Gustafsson, T. Jogestrand, I. Hafström, J. Frostegård, Diet and fatty acid pattern among patients with SLE: associations with disease activity, blood lipids and atherosclerosis, Lupus 21 (2012) 1405–1411, https://doi.org/10.1177/0961203312458471.
[66] Y. Minami, Y. Hirabayashi, C. Nagata, T. Ishii, H. Harigae, T. Sasaki, Intakes of vitamin B6 and dietary fiber and clinical course of systemic lupus erythematosus: a prospective study of Japanese female patients, J. Epidemiol. 21 (2011) 246–254, https://doi.org/10.2188/jea.je20100157.
[67] S.A. Jenks, K.S. Cashman, E. Zumaquero, U.M. Marigorta, A.V. Patel, X. Wang, D. Tomar, M.C. Woodruff, Z. Simon, R. Bugrovsky, E.L. Blalock, C.D. Scharer, C. M. Tipton, C. Wei, S.S. Lim, M. Petri, T.B. Niewold, J.H. Anolik, G. Gibson, F.E.-H. Lee, J.M. Boss, F.E. Lund, I. Sanz, Distinct effector B cells induced by unregulated toll-like receptor 7 contribute to pathogenic responses in systemic lupus erythematosus, Immunity 49 (2018) 725–739.e6, https://doi.org/10.1016/j.immuni.2018.08.015.
[68] S. Caielli, D.T. Veiga, P. Balasubramanian, S. Athale, B. Domic, E. Murat, R. Banchereau, Z. Xu, M. Chandra, C.-H. Chung, L. Walters, J. Baisch, T. Wright, M. Punaro, L. Nassi, K. Stewart, J. Fuller, D. Ucar, H. Ueno, J. Zhou, J. Banchereau, V. Pascual, A CD4(+) T cell population expanded in lupus blood provides B cell help through interleukin-10 and succinate, Nat. Med. 25 (2019) 75–81, https://doi.org/10.1038/s41591-018-0254-9.